MCP Papers in Press. Published on July 5, 2017 as Manuscript M116.064923

STUDY OF THE PLASMA MEMBRANE PROTEOME DYNAMICS REVEALS NOVEL TARGETS OF THE NITROGEN REGULATION IN YEAST

Jennifer Villers, Jérôme Savocco, Aleksandra Szopinska, Hervé Degand, Sylvain Nootens and Pierre Morsomme
Université catholique de Louvain, Institut des Sciences de la Vie, Croix du Sud 4-5, B-1348 Louvain-la-Neuve
Corresponding author: pierre.morsomme@uclouvain.be

RUNNING TITLE

Impact of nitrogen sources on yeast plasma membrane proteome

ABBREVIATIONS

Abbreviation	Definition
NCR	Nitrogen Catabolite Repression
ART	Arrestin-Related Trafficking adaptors
MCC	Microdomains Containing Can1
TORC1	Tor Complex 1

ABSTRACT

Yeast cells, to be able to grow on a wide variety of nitrogen sources, regulate the set of nitrogen transporters present at their plasma membrane. Such regulation relies on both transcriptional and post-translational events. While microarray studies have identified most nitrogen-sensitive genes, nitrogen-induced post-translational regulation has only been studied for very few proteins among which the general amino acid permease Gap1. Adding a preferred nitrogen source to proline-grown cells triggers Gap1 endocytosis and vacuolar degradation in an Rsp5-Bul1/2-dependent manner. Here, we used a proteomic approach to follow the dynamics of the plasma membrane proteome after addition of a preferred nitrogen source. We identified new targets of the nitrogen regulation and four transporters of poor nitrogen sources—Put4, Opt2, Dal5 and Ptr2—that rapidly decrease in abundance. Although the kinetics is different for each transporter, we found that three of them—Put4, Dal5 and Ptr2— are endocytosed, like Gap1, in an Rsp5-dependent manner and degraded in the vacuole. Finally, we showed that Gap1 stabilization at the plasma membrane, through deletion of Bul proteins, regulates the abundance of Put4, Dal5 and Ptr2.

Keywords: yeast plasma membrane, proteomics, nitrogen sources, transporters, endocytosis, arrestin

INTRODUCTION

Yeast cells can grow on a wide variety of nutrients and rapidly adapt to changes in nutrient availability by remodeling the composition of their plasma membrane. This remodeling process involves a fine tuning of gene expression, transcript regulation, and protein post-translational regulation and trafficking. One example that has been extensively studied is the adaptation of yeast cells to different sources of nitrogen. Yeast cells can use various nitrogen sources as the unique source of all the cellular nitrogen. This ability requires permeases for the transport of those compounds and enzymes for their catabolism leading to generation of ammonium or glutamate. Once inside the cell, ammonium can react with α-ketoglutarate, provided by carbon metabolism, to produce glutamate, and can react with glutamate to produce glutamine. All the nitrogenous compounds in the cell are synthesized from either glutamate or glutamine (1). Yeast cells provided with an appropriate source of carbon and nitrogen can synthesize all L-amino acids used in protein synthesis (2). The sources of nitrogen can be classified as preferred and non-preferred. Preferred nitrogen sources are easier to convert into glutamate and glutamine, support rapid cell growth and repress the transcription of genes encoding proteins necessary for the uptake and catabolism of less preferred nitrogen sources, reviewed in (1, 3, 4). This gene regulation called nitrogen catabolite repression (NCR) primarily functions to restrain the yeast's capacity to use non-preferred nitrogen sources when preferred ones are available. In the absence of a preferred nitrogen source, the general derepression of NCR-regulated genes enables cells to indiscriminately scavenge alternative, non-preferred nitrogen sources. The criteria to judge the quality of a particular nitrogen source are the growth rate and the ability to repress or not the pathways for utilization of less preferred nitrogen sources. Commonly used preferred nitrogen sources for *S. cerevisiae* are ammonium, glutamine and asparagine. The non-preferred nitrogen source used in most studies about yeast nitrogen regulation is proline. Notably, the classification of nitrogen sources is not absolute, and their repressive effects can vary significantly between different yeast strain backgrounds. For example, ammonium is a repressing nitrogen source for CEN.PK and Σ1278b-

derived stains, whereas it is not for many S288c-derived strains, even though it promotes high rates of growth (4).

Hundreds of genes show differences in their expression according to the nature of the nitrogen source available in the extracellular environment. Several global studies based on microarrays have been conducted to identify all the genes having a level of expression sensitive to NCR (5-7). According to these transcriptomic studies, many genes encoding transporters of compounds that can be used as source of nitrogen are sensitive to NCR. In addition, a recent study showed accelerated degradation of some NCR transcripts when a nitrogen source is added to nitrogen-limited cultures, revealing an additional layer of mRNA regulation (8). Although high levels of mRNA usually result in high amounts of protein, the general correlation between mRNA and protein abundance is often poor (9). The abundance and stability of proteins are also determined by complex posttranslational processes, such as protein turnover rate, covalent protein modifications and subcellular relocalization. For these reasons, there is a great need for direct measurements of protein levels. Targeted approaches, such as Western blot or microscopy, are commonly used to measure the abundance and localization of specific proteins of interest. Using specific transport assays, Grenson and colleagues showed that the general amino acid permease Gap1, the proline permease Put4 and the allantoate permease Dal5 are subjected to a posttranslational regulation that suppresses their transport activity within one hour after addition of ammonium to proline-grown cultures (10). Further in-depth studies focused on the general amino acid permease Gap1 unraveled the precise mechanism of Gap1 post-translational regulation (11-15). In cells grown with proline as unique nitrogen source, *GAP1* gene is highly expressed and newly synthesized protein accumulates at the plasma membrane in an active and stable form (14). When a preferred nitrogen source is added to proline-grown cultures, *GAP1* transcription is repressed and any Gap1 already present at the plasma membrane is rapidly ubiquitylated in an Rsp5-dependent fashion, endocytosed and degraded in the vacuole (11, 16). Gap1 ubiquitylation occurs on two lysine residues in the cytosolic N-terminus (K9 and K16) and requires the

activity of at least one of the two redundant ubiquitin ligase adaptors Bul1 and Bul2 (13). Bul1 and Bul2 are members of the arrestin-related trafficking (ART) adaptor family. ART proteins are recognized through their PY motifs by Rsp5 WW domains, and mediate the interaction between Rsp5 and the plasma membrane protein that must be ubiquitylated, here Gap1 (13, 15, 17). In the presence of a preferred nitrogen source, Rsp5-Bul1/2-dependent ubiquitylation of Gap1 is also required for direct sorting of the newly synthesized protein from the late secretory pathway to the vacuole without passing through the plasma membrane (13, 17). In proline-grown cells, the protein kinase Npr1 is required for stabilization of Gap1 at the plasma membrane (14). Npr1 promotes phosphorylation of the ubiquitin ligase adaptors Bul1 and Bul2. When phosphorylated, Bul adaptors bind to the 14-3-3 proteins, hence preventing Rsp5-Bul1/2-dependent ubiquitylation of Gap1. This inhibition can be lifted by addition of a preferred nitrogen source (15). Although that kind of studies has resulted in a tremendous increase in our knowledge of the cellular response to changes in nutrient availability, these techniques only allow to study a very limited number of proteins, hence opening a tiny window into the complexity of the proteome regulation. This emphasizes the need for techniques that enable the direct analysis of large sets of proteins in order to reveal global regulation mechanisms. In this context, mass spectrometry-based proteomics has emerged as the technology of choice for studying complex proteomes. This technique allows not only identification of proteins, but also quantitative comparisons of the relative abundance of proteins under different conditions (18, 19).

Here, we used a mass spectrometry-based proteomic approach to follow the dynamics of the plasma membrane proteome after the addition of a preferred nitrogen source to proline-grown cells. We identified (1) new targets of the nitrogen regulation, (2) four transporters of poor nitrogen sources—Put4, Opt2, Dal5 and Ptr2—that rapidly decrease in abundance. Although the kinetics is different for each transporter, we found that three of them—Put4, Dal5 and Ptr2— are endocytosed, like Gap1, in an Rsp5-

dependent manner and degraded in the vacuole. (3) Finally, we showed that Gap1 stabilization at the plasma membrane, through deletion of Bul proteins, regulates the abundance of Put4, Dal5 and Ptr2.

EXPERIMENTAL PROCEDURES

Yeast strains and growth conditions

Yeast strains are listed and detailed in Table S1. Strains used for proteomic experiment and validation by immunodetection (Table 1, Figures S1, S4, 1A and 1B) are derivatives of the CEN.PK113-7D strain, kindly provided by Prof. P. Kötter, Frankfurt, Germany. Other strains used in this study are derivatives of the BY4741/2 strains. The *npi1* mutant strain was kindly provided by Prof. B. André, Brussels, Belgium. The strain was obtained by insertion of a selective marker in the *RSP5* promoter, which results in an attenuated *RSP5* gene expression. The *9-arrestin*Δ, *9-arrestin*Δ *bul1*Δ and *9-arrestin*Δ *bul1*Δ *bul2*Δ strains were kindly provided by Prof. H. Pelham, Cambridge, UK. The *bul1*Δ *bul2*Δ double deletion strain was isolated from crossing of *bul1*Δ with *bul2*Δ, followed by sporulation and tetrad dissection, all initial strains coming from Euroscarf. Strains containing a 9-myc-labeled version of Put4, Ptr2 or Qdr3 were isolated by insertion of a DNA fragment amplified by PCR using as a template pYM18 and pYM19 plasmids from Euroscarf containing *kanMX* resistance gene and *HIS3* auxotrophic marker, respectively. Strains containing a 9-myc-labeled version of Put4 with the auxotrophic *URA3* marker were isolated by insertion of a DNA fragment amplified by triple PCR using as templates pYM18 and pRS316 plasmids. *PUT4-9MYC bul1*Δ *bul2*Δ *pep4*Δ and *PUT4-9MYC bul1*Δ *bul2*Δ *gap1*Δ triple deletion strains were obtained by crossing of the *PUT4-9MYC bul1*Δ *bul2*Δ strain with *pep4*Δ and *gap1*Δ yeast strains from Euroscarf, respectively. All auxotrophic strains were transformed with pRS316 *URA3* and/or pFL36 *HIS3, LEU2, MET15 or LYS2* plasmids in order to make them prototrophic and able to grow on minimal proline-containing medium (Table S1). Yeast cells were grown in minimal medium containing 2% (w/v) glucose, 0.7% (w/v) Yeast Nitrogen Base w/o amino acids and ammonium sulfate and 0.1% (w/v) proline as unique source of nitrogen. The change in nitrogen source was operated by addition of 10 mM ammonium or glutamine in proline-grown cultures for 0, 15, 45 and 90 minutes.

Plasmids

The plasmids used in this work are listed in Table S2. For pRS316 *GAP1-PTR2-YFP*, *GAP1-MEP2-YFP*, and *GAP1-QDR3-YFP* plasmids, DNA fragments containing *PTR2-*, *MEP2-* or *QDR3-YFP* were amplified by triple PCR using as templates *PTR2*, *MEP2* and *QDR3* ORF from CEN.PK113-7D and *YFP* ORF from the pYM39 Euroscarf plasmid. Amplified fragments were cloned by gap-repair in yeast into a pRS316 vector containing the *GAP1* promoter, previously digested with AgeI, kindly provided by Prof. C. Govaerts, Brussels, Belgium (20). The plasmids encoding Gap1-GFP, Bul1 and Bul1$^{PPSY>AASY}$ were kindly provided by Prof. Bruno André, as well as the pFL36 *HIS3 LEU2 MET15 or LYS2* plasmids.

Yeast cell extracts

Yeast cells were harvested at an $O.D._{600}$ of 3, which equals 2.10^7 cells/ml. Plasma membrane enriched fractions were prepared as previously described (21). Yeast crude membrane extracts were prepared as previously described (22), except that no dithiothreitol was added. Yeast total cell extracts were prepared as previously described (23), except that cells were resuspended in 200 µl of cold homogenization medium (250 mM sorbitol, 50 mM imidazole, 1 mM $MgCl_2$, pH 7.5) containing a protease inhibitor mix (1 mM PMSF and 2 µg/ml each of leupeptin, aprotinin, antipain, pepstatin and chymostatin) before breaking. The protein concentration was then determined using Bicinchoninic assay, as previously described (24).

Antibodies and immunoblotting

Yeast cell extracts were mixed with an equal volume of sample buffer (100 mM Tris-HCl, pH 6.8, 4 mM EDTA, 4% SDS, 20% glycerol, 0.002% bromophenol blue) containing 1% DTT and incubated at room temperature for 10 minutes. Proteins were resolved by SDS-PAGE and transferred to a PVDF membrane using a Trans-Blot® Turbo™ Transfer System and Mini PVDF Transfer Packs (Bio-Rad). Proteins were immunodetected as previously described (21). Primary antibodies used in this work and their

corresponding dilutions are listed in Table S3. Primary rabbit polyclonal antibodies against Opt2 and Dal5 were produced for this study by Thermo Scientific, and were raised against a synthetic peptide designed specifically for each protein (Opt2, residues 105-123, sequence DQYEEWKRLVDLEDLDSKE; Dal5, residues 524-543, sequence ENLEFSDLTDFENPNFRYTL). Western blots were quantified using Fiji software (based on Image J software) and statistical analyses were performed using JMP Statistical Software.

Proteomics: experimental design and statistical rationale

To compare the proteome of yeast cells grown overnight in ammonium vs. proline, four independent biological replicates were analyzed. For each biological replicate, yeast cells were grown in parallel and plasma membranes were enriched at the same time to reduce variability coming from growth conditions or from the enrichment procedure. The same protocol was applied for the kinetics experiment where each culture treated with ammonium was grown and extracted together with one control (proline) culture. This procedure was repeated three times for each time point, resulting in a total of three biological replicates for each time point.

Protein digestion and iTRAQ labeling

Purified plasma membranes (20 μg of protein) were solubilized in 50 mM TEAB, 0.1 % Rapigest (Waters), pH 8.0, by sonication for 5 min in a bath sonicator (Bioruptor, Diagenode), and the proteins reduced by incubation for 1 h at 60°C with 25 mM tris(2-carboxyethyl)phosphine, then alkylated with 0.26 M methyl-methanethiosulfonate (MMTS) for 10 min at room temperature in the dark. The reduced and alkylated proteins were digested for 16 h at 37°C using sequencing grade modified trypsin (Promega) at a protease/protein ratio of 1/20 and the Rapigest lysed by incubating the protein sample in 0.5% trifluoroacetic acid (TFA) for 60 min at 37°C. After centrifugation of the sample at 54000 rpm (TLA55, Optima-Beckman) for 45 min at 4°C, the supernatant was centrifuged for 20 min at 54000 rpm (TLA55,

Optima-Beckman), then the final supernatant was vacuum dried (Speedvac SC 200, Savant) and iTRAQ labeling performed according to the manufacturer's protocol (Applied Biosystems).

Reversed phase chromatography

Before separation, the samples were resuspended in 0.025% TFA and 5% acetonitrile (ACN), then the labeled peptides were mixed together and 12.9 µg of the mixture desalted using a C18 Pep Map 100 pre-column and subjected to reverse phase chromatography on a C18 PepMap100 (LC Packings) analytical column for 180 min at a flow rate of 300 nl/min using a linear gradient from 8% ACN in water/0.1% TFA to 76% ACN in water/0.085% TFA. The eluted peptides were mixed with α-cyano-4-hydroxycinnamic acid matrix (2 mg/ml in 70% ACN, 0.1% TFA) and spotted directly onto a MALDI target using a Probot system (LC Packings Amersham).

Mass spectrometry analysis

The spotted plate was analyzed on an Applied Biosystems 4800 MALDI TOF/TOF Analyzer using a 200 Hz solid state laser operating at 355 nm. MS spectra were obtained using a laser intensity of 3200 and 2000 laser shots per spot in the m/z range of 800 to 4000, while MS/MS spectra were obtained by automatic selection of the 12 most intense precursor ions per spot using a laser intensity of 3800 and 2100 laser shots per precursor. Collision-induced dissociation was performed with an energy of 1 kV with air as the collision gas at a pressure of 1 x 10^6 Torr. Data were collected using Applied Biosystems 4000 Series Explorer™ software. LC/MSMS data were processed using ProteinPilot software and the Paragon™ search algorithm (Shilov et al., 2007) (Applied Biosystems/MDS SCIEX/4800 v4.0). The mass spectrometry proteomics data have been deposited to the ProteomeXchange Consortium via the PRIDE partner repository with the dataset identifier PXD005273.

Protein identification

The MS/MS data were used to search the UniProtKB/Swiss-Prot database (276 256 sequences Release 54.0 of 24, July 07 from the website http://www.ebi.ac.uk/FTP/) using the "thorough search" option and a *S. cerevisiae* taxonomy filter. MS and MS/MS tolerances were set to 0.15 and 0.4 Da, respectively. The "iTRAQ 4plex peptide labeled" or "iTRAQ 8plex peptide labeled" sample types and a "biological modification ID focus" were selected in the analysis method. Trypsin was selected as the digestion enzyme with allowance for a single missed cleavage, and cysteine alkylation by MMTS as a modification. The results were further processed by the Pro Group™ Algorithm to determine the minimal set of justifiable identified proteins. Proteins were annotated based on Saccharomyces Genome Database, Gene Bank, and UniProt Databases.

All reported data were based on 99% confidence for protein identification as determined by ProteinPilot (ProtScore ≥ 2.0). Protein identification confidence was expressed as the "Unused Protein Score", a measurement of the protein identification confidence taking into account peptides from spectra that have not already been "used" by higher scoring proteins. Quality of identification was assessed by false discovery rate analysis. The FDR analysis provided by ProteinPilot consists of a target-decoy database search. The number of decoy proteins relative to the number of target proteins reported by the search was lower than 1% for each run.

Quantification of relative change

To determine differences in protein abundance, the average ratio of the identified protein was calculated by ProteinPilot based on the log ratios of the peptides. Peptides that matched multiple proteins were not included in the quantification by the software. Background correction was applied to avoid biasing iTRAQ ratios towards unity and extreme ratios were set to an upper limit of 100-fold. Data were normalized to

correct for unequal mixing of labeled peptides, based on the assumption that most proteins do not change in abundance. The bias correction algorithm calculates the median average protein ratio, corrects it to unity, and then applies this factor to all quantitation results. Differentially expressed proteins were further analyzed for significant down- or upregulation by comparing protein log ratios to zero using a one-sample *t*-test with df degrees of freedom, where $df = sample\ size - 1$ (i.e. the number of peptides used for protein quantification -1).

$$t = \frac{average\ of\ \log ratios}{standard\ error}$$

An important limitation of *t*-tests when sample size is small is that fewer observations lead to difficulties in accurately determining the standard error, making the denominator of the *t*-test unreliable. To avoid large *t*-scores arising because of small standard errors coming from few peptide ratios, ProteinPilot corrects the denominator of the *t*-test as follows:

$$\max\left[\frac{s}{\sqrt{n}}, \frac{0.17}{\sqrt{n}}, log_{10}(1.15)\right]$$

with s being the standard deviation of log ratios and n the sample size.

Another important limitation of *t*-tests is the absence of correction for multiple testing. To establish the list of differentially abundant proteins, we calculated a single p-value for each protein and applied Bonferroni correction for multiple testing. We used two different methods to compute the single p-value. In the first method, we pooled the peptide ratios coming from the different biological replicates and used the *t*-test described above on the pooled peptide ratios. In the second method, we combined the p-values computed by ProteinPilot using weighted z-scores (25-27). The workflow is the following:

(1) two-sided p-values are converted into one-sided p-values according to the direction of change

$P_{one-sided} = P_{two-sided}/2 \qquad if\ ratio < 1$

$P_{one-sided} = 1 - P_{two-sided}/2 \qquad otherwise$

(2) one-sided p-values are converted into z-scores (Z_i) using the qnorm function in R

(3) z-scores (Z_i) are combined together using the following equation

$$Z = \frac{\sum_{i=1}^{k} w_i Z_i}{\sqrt{\sum_{i=1}^{k} w_i^2}}$$

with weight $w_i = \sqrt{n_i}$, n_i being the sample size, and k the number of biological replicates.

(4) the combined z-score (Z) is then converted into a two-sided p-value using the pnorm function in R

$$P_{two-sided} = pnorm\left(-abs(Z)\right) * 2$$

P-values that were reported as 0.0000 by ProteinPilot (Table S5) were arbitrarily set to 0.0001 to allow the calculation of a combined p-value. A cutoff level of significance of 95% (or $P_{two-sided}$ < 0.05) after Bonferroni correction was chosen as a criterion for each protein.

Fluorescence microscopy

Cells expressing Gap1-GFP, Ptr2-YFP, Mep2-YFP or Qdr3-YFP were cultivated as described above, laid down on a thin layer of 1% agarose and viewed at room temperature with a Leica DMR epifluorescence microscope with a 100x oil immersion objective and GFP or FITC fluorescence light filters. Image acquisition time may vary from one image to another. No contrast enhancement was applied.

q-RT-PCR

Total RNA was extracted and analyzed by quantitative real-time PCR as previously described (23). Oligonucleotides designed for real-time PCR are listed in Table S4. Relative expression levels were determined with efficiency correction (28).

RESULTS

The abundance of 27 plasma membrane proteins varies according to the nitrogen source

To determine the influence of the nitrogen source on yeast cell surface proteins, we compared the plasma membrane proteomes of wild-type yeast cells supplied with a non-preferred nitrogen source (proline) and of cells supplied with a preferred nitrogen source (ammonium). The wild-type prototrophic yeast strain CEN.PK113-7D was used in this experiment, allowing the use of a unique nitrogen source in the medium. We prepared plasma membrane enriched fractions from yeast cells grown overnight either in the presence of proline or ammonium. This procedure includes one step of differential centrifugation to pellet crude membranes, one step of acidic precipitation to selectively precipitate contaminant membranes while recovering plasma membrane proteins in the supernatant, and one step of membrane stripping to remove peripheral membrane proteins without affecting integral components. We assessed the quality of the enrichment procedure by comparing the relative enrichment of Pma1, the plasma membrane H^+-ATPase, with that of markers of the endoplasmic reticulum (Sec22), Golgi apparatus (Emp47), endosomes (Pep12), vacuole (Vph1), and cytosol (Cdc48) (Figure S1A). Proteins in the plasma membrane enriched fraction were digested with trypsin and peptides were labeled using isobaric tags for relative and absolute quantitation (iTRAQ). We performed a gel-free quantitative mass spectrometry analysis in order to identify and quantify plasma membrane proteins, and determine how their relative abundance is affected by the two different nitrogen sources. Plasma membrane enrichment was further confirmed by the relative abundance of peptides originating from plasma membrane proteins (50%) compared to other organelles (Figure S1B). Plasma membrane proteins were identified based on a higher number of peptides than contaminant proteins and most contaminant peptides were from cytosolic or ribosomal proteins. Likewise, we showed in figure S1A that this enrichment procedure allows to efficiently reduce the abundance of proteins originating from internal membranes such as endosomes, endoplasmic reticulum and Golgi. Accordingly,

we can consider that protein variations observed by mass spectrometry on plasma membrane enriched fractions directly reflects protein variations at the plasma membrane.

The changes in plasma membrane protein abundance associated with nitrogen sources were determined by comparing the protein abundance ratios (ammonium-grown cells / proline-grown cells) in four independent biological replicates. Only proteins identified with an unused protein score ≥ 2.0 (identified with at least one 99% confidence peptide) were considered for further analysis. Using this selection criterion, we identified a total of 117 plasma membrane proteins (Table S5), which accounts for almost half of the total number of plasma membrane proteins reported in databases (245 proteins in Saccharomyces Genome Database and 239 in Organelle Database). These databases report protein subcellular localization from the peer-reviewed literature and from large-scale studies of protein localization. Among the 117 plasma membrane proteins identified in this study, 66% were integral plasma membrane proteins, 19% were lipid-anchored proteins, and 15% were peripheral proteins tightly associated to the plasma membrane. Among integral plasma membrane proteins, 47 were plasma membrane transporters. According to YTPdb (29), a total of 139 transporters are localized at the plasma membrane, meaning that we identified approximately one third of them.

For each protein in each biological replicate, a protein ratio (ammonium-grown cells / proline-grown cells) and a p-value assessing whether this ratio can be considered as different from unity or not was computed using the ProteinPilot software (Table S5). The p-value calculation, based on a one-sample *t*-test, is described in the experimental procedure. Raw data at the peptide level can be found in Table S6. To assess the reproducibility of the quantitation, we did a pairwise comparison between protein log ratios from the four biological replicates (Figure S2). The pairwise comparison was concordant among replicates, with Pearson correlation coefficients ranging from 0.62 to 0.88. To identify differentially abundant proteins, we calculated a single p-value combining results from the four biological replicates. To do so, we used two different methods that gave comparable results. The first method consists, for each protein, in pooling

peptide ratios coming from the four biological replicates and computing a single p-value using a one sample *t*-test. This methodology assumes a common effect size and direction among samples, which is appropriate when different samples are taken from similar populations (26, 27). Second, we used a meta-analysis method to combine the p-values computed for each biological replicate by ProteinPilot. In a recent article, Pascovici and colleagues suggested that combining ratio p-values could be a suitable and pragmatic approach to analyze multi-run iTRAQ experiments (30). They propose to combine p-values using a statistical meta-analysis called the Stouffer method. In this method, individual p-values are converted into z-scores, z-scores (Z_i) are then combined using the following formula:

$$Z = \frac{\sum_{i=1}^{n} Z_i}{\sqrt{n}}$$

and the combined z-score (Z) is converted back into a p-value using the normal distribution function. One important limitation of this method is that the combined p-value does not take into account the direction of change of the protein ratio. One protein could have a ratio significantly higher than one in one biological replicate and significantly smaller than one in another replicate. The combined p-value would be low, but the ratio inconsistent. To circumvent this, the authors proposed to add a ratio trend consistency measure that would exclude proteins having inconsistent protein ratios from the list of differentially abundant proteins. Here, we implemented a method first described by Liptak and later completed by Whitlock and Zaykin that (1) takes into account the direction of change of the protein ratio, and (2) weights the different z-scores according to the sample size, i.e. the number of peptides used to compute the p-value of a protein ratio (25-27). The details of the calculations are presented in the experimental procedures.

After Bonferroni correction for multiple testing, 27 plasma membrane proteins were identified as differentially abundant in both methods (27 in the analysis on pooled peptides and 29 in the meta-analysis). Differentially abundant proteins are listed in Table 1. Volcano plots showing significance against fold-change are presented in Figure S3A, and the correlation between p-values computed using the two

different methods is presented in Figure S3B. For 23 hits out of the 27, the abundance was higher in cells supplied with proline. Among these, we found several transporters of nitrogenous compounds previously described as NCR-sensitive: the general amino acid permease Gap1, the oligopeptide transporter Opt2, the allantoate permease Dal5, the ammonium permease Mep2, the urea and polyamine transporter Dur3, and the peptide transporter Ptr2. We also found the plasma membrane H^+-ATPase Pma1, the multidrug transporter Qdr3, components of eisosomes and microdomains containing Can1 (MCCs) (Pil1, Lsp1, Nce102, Sur7 and Ycp4), proteins involved in cell wall integrity (Gas3, Gas5 and Gsc2), the plasma membrane t-SNARE Sso2, one protein involved in lipid metabolism (Plb1), the GTP-binding protein Ras2, two GTPases (Rho3 and Gpa2), one kinase (Yck2) and a GPI-anchored protein of unknown function (Ecm33). Conversely, only 4 hits out of the 27 were more abundant in ammonium-grown cultures: the histidine permease Hip1, the methionine permease Mup1, the glucose transporter Hxt4, and the ABC transporter Pdr5. As a control, we confirmed the MS data on several targets by immunodetection in fractions enriched in plasma membrane proteins (Figure S4A) and on total cell extracts (Figure S4B). Interestingly, Pma1 and Nce102 signals from ammonium-grown cells were decreased in plasma membrane enriched fractions, while they remained stable in total cell extracts, suggesting that these proteins are internalized and not degraded. In addition, we monitored by immunodetection the abundance variation of the proline transporter Put4. The gene coding for Put4 is a known NCR target and the two peptides belonging to Put4 identified in our proteomic screening were more abundant in proline-grown cells. Although the number of peptides was too low to allow statistically reliable quantification, we were able to confirm this abundance variation by immunodetection in total extracts.

The abundance of different plasma membrane proteins varies at different rates after addition of ammonium to proline-grown yeast cells

As the variations in protein amounts observed in the steady-state mass spectrometry experiment could reflect transcriptional, translational, as well as post-translational regulation, we analyzed the temporal evolution (up to 90 minutes) of the plasma membrane proteome of proline-grown yeast cells upon the addition of 10 mM ammonium. Interestingly, different plasma membrane proteins decreased in abundance with different kinetics (Figure 1A). For instance, the abundance of the general amino acid permease Gap1, of the proline permease Put4, and of the oligopeptide transporter Opt2 decreased by 50% within 15 minutes. The decrease in abundance of Dal5 and Ptr2 was apparent 45 and 90 minutes, respectively, after the addition of ammonium. Other proteins, such as Nce102, identified in our screening remained stable within the 90 minutes time window.

Based on these results, we hypothesized that plasma membrane proteins decreasing in abundance within 90 minutes undergo endocytosis, leading finally to vacuolar degradation. Consistent with this hypothesis, we observed the same decrease in abundance over time in total cell extracts (Figure 1B), suggesting protein disappearance rather than subcellular relocalization. In order to follow their trafficking *in vivo*, plasma membrane proteins were fused to Green and Yellow fluorescent proteins (GFP and YFP) and expressed under the control of the *GAP1* promoter. The *GAP1* promoter has the advantage to ensure high gene expression in proline-containing cultures, and is sensitive to NCR. As a result, the addition of a preferred nitrogen source to proline-grown cells induced the catabolic repression of the fluorescently labeled proteins and their fate could be followed over time in microscopy (Figure 1C). Experiments requiring gene modification or plasmid insertion were performed in auxotrophic yeast strains of the BY background supplemented with plasmids containing the missing auxotrophic markers. As ammonium does not induce NCR in BY background yeast cells (4), we chose glutamine as preferred nitrogen source. Hence, the addition of glutamine to proline-grown cells triggered a rapid decrease of Gap1-GFP fluorescence

intensity at the plasma membrane, along with the appearance of fluorescent dots inside the cell—most likely endosomes—and a rapid staining of the vacuole (45 min). For Ptr2-YFP, we observed fluorescent dots inside the cell after 15 minutes, and a delayed vacuolar staining (90 min) compared to Gap1-GFP, which is consistent with the hypothesis of a slower endocytic process. Qdr3-YFP and Mep2-YFP remained stable at the plasma membrane within the 90 minute time window, and were therefore used as negative controls. Other target proteins were mislocalized when fused to YFP, and consequently not analyzed in microscopy. To further validate the hypothesis of a vacuolar degradation, we compared the protein amounts of Gap1, Put4-9myc, Dal5 and Ptr2-YFP in a wild-type strain and in a *pep4*Δ strain deleted for the vacuolar protease Pep4 (Figure 1D). While the addition of glutamine to proline-grown BY background wild-type cells triggered a similar decrease in protein amounts, this decrease was severely impaired in *pep4*Δ mutant cells, which is consistent with the hypothesis of vacuolar degradation.

Together, our results suggest that at least four plasma membrane transporters—Gap1, Put4, Dal5, Ptr2—undergo endocytosis and vacuolar degradation with different kinetics after the addition of a preferred nitrogen source to proline-grown cells. We expected a similar mechanism for Opt2, but were not able to confirm this hypothesis due to the poor quality of anti-Opt2 antibodies. Conversely, proteins remaining stable within the 90 minutes time window were more likely subject to a transcriptional regulation, such as NCR.

The degradation of Gap1, Put4, Dal5 and Ptr2 requires the ubiquitin ligase Rsp5

Above results suggest that the addition of a preferred nitrogen source to proline-grown wild-type yeast cells triggered internalization and vacuolar degradation of the plasma membrane proteins Gap1, Put4, Dal5 and Ptr2. The mechanism of internalization of the general amino acid permease Gap1 has been widely studied (11-15). Gap1 internalization requires the ubiquitin ligase Rsp5 and at least one of the two functionally redundant adaptor proteins Bul1 and Bul2. First, we asked the question whether Rsp5 is

involved in the degradation of transporters showing a rapid decease in abundance (< 90 min) after addition of a preferred nitrogen source to proline-grown cells. To answer this question, we used a BY background yeast strain deficient for *RSP5* gene expression (*npi1*), and compared the protein amounts in wild-type and *npi1* cells upon addition of glutamine. Using immunodetections, we showed that the degradation of Gap1, Put4-9myc, Dal5 and Ptr2-YFP requires normal levels of *RSP5* expression (Figure 2A). These results were confirmed in fluorescence microscopy, where Ptr2-YFP was sequestered at the plasma membrane in the absence of Rsp5 after addition of glutamine (Figure 2B). The latter suggesting that Rsp5 is required for the internalization step. Note that Put4 and Dal5 have been previously shown to be inactivated for their transport activity in an Rsp5-dependent manner after addition of ammonium to proline-grown cultures (10, 31). Additionally, it is interesting to note that Put4-9myc and Dal5 protein levels were reduced by a factor of 3 in *npi1* cells compared with wild-type cells, while Ptr2-YFP protein levels remained stable and Gap1 protein levels were increased (Figure 2).

Loss of Bul1 and Bul2 function results in very low levels of Put4, Dal5 and Ptr2 proteins

Since Put4, Dal5 and Ptr2 transporters are degraded in an Rsp5-dependent manner, like Gap1, we questioned the role of Bul1 and Bul2 ubiquitin ligase adaptors in this process. To do so, we quantified the protein levels of Gap1, Put4-9myc, Dal5 and Ptr2-YFP in total cell extracts before and after the addition of a preferred nitrogen source to proline-grown WT and *bul1*Δ *bul2*Δ cells. In this experiment, we found (1) that neither Bul1 nor Bul2 are required for Put4-9myc, Dal5 and Ptr2-YFP endocytosis, and (2) that the levels of Put4-9myc and Dal5 were reduced by at least a factor of 5 in *bul1*Δ *bul2*Δ cells compared with wild-type cells, Ptr2-YFP protein levels were reduced by a factor of 3, while Gap1 protein levels remained stable (Figure 3A). We observed similar low protein levels in the *9-arrestin*Δ *bul1*Δ *bul2*Δ yeast strain deleted for eleven of the twelve proteins of the ART family known so far (32), but not in the *9-arrestin*Δ *bul1*Δ strain (expressing a functional Bul2 protein), the *9-arrestin*Δ strain (expressing both Bul1 and Bul2

proteins), *bul1*Δ or *bul2*Δ single deletion strains (Figure 3B). To further confirm that this effect on protein levels is specific to Bul proteins, we complemented the *bul1*Δ *bul2*Δ strain with a plasmid expressing FLAG-tagged wild-type Bul1, and hence restored Put4-9myc and Dal5 proteins to normal levels (Figure 3C). While the expression of wild-type Bul1 was able to rescue the *bul1*Δ *bul2*Δ strain, a mutant Bul1 with altered PY motif (PPSY>AASY) failed to do so (Figure 3C). The degradation profile of Gap1 after addition of glutamine was used as a control for Bul1 activity. As expected, Gap1 was readily degraded in the *bul1*Δ *bul2*Δ strain complemented with wild-type Bul1, while it remained stable in cells expressing the mutant form of Bul1. Using antibodies raised against FLAG tag, we showed that the protein levels of the wild-type and mutant forms of Bul1 are comparable, confirming that the low Put4 and Dal5 protein levels observed in cells expressing Bul1$^{PPSY>AASY}$ are due to the absence of PY motif rather than to a deficient expression or premature degradation of Bul1$^{PPSY>AASY}$. Together, our results suggest that at least one of the ubiquitin ligase adaptors Bul1 or Bul2 is required to maintain normal Put4, Dal5 and Ptr2 protein levels in proline-containing medium, and that this function relies on their PY motif.

Note that Put4-9myc and Dal5 were still degraded after the addition of a preferred nitrogen source to proline-grown *bul1*Δ *bul2*Δ, *9-arrestin*Δ and *9-arrestin*Δ *bul1*Δ mutant strains. This suggests that Bul1 and Bul2 are either not involved in the endocytosis and degradation of these proteins, or that they function redundantly with other ubiquitin ligase adaptors to mediate their endocytosis.

Loss of Bul1 and Bul2 function results in vacuolar degradation of Put4, Dal5 and Ptr2

To explain the low protein levels of Put4, Dal5 and Ptr2 in the *bul1*Δ *bul2*Δ strain, we first tried to assess whether the low protein abundance is due to a low level of expression of the corresponding genes. To do so, we compared the mRNA levels of *PUT4*, *DAL5* and *GAP1* genes in wild-type and *bul1*Δ *bul2*Δ yeast strains by quantitative real-time polymerase chain reaction (q-RT-PCR) (Figure 4A). Although we observed a general 50% decrease of *PUT4*, *DAL5* and *GAP1* gene expression in the *bul1*Δ *bul2*Δ strain, this difference

is not enough to explain the low protein levels. Especially since the *GAP1* gene is regulated similarly to *PUT4* and *DAL5*, while their corresponding protein levels differ markedly. To determine whether Put4, Dal5 and Ptr2 are degraded in the absence of Bul1 and Bul2, we used a triple mutant yeast strain deleted for Bul1, Bul2 and the vacuolar peptidase Pep4 (*bul1*Δ *bul2*Δ *pep4*Δ), and compared the relative protein levels in this strain and in *bul1*Δ *bul2*Δ (Figure 4B). We observed strong increases of Put4-9myc (9-fold), Dal5 (8-fold) and Ptr2-YFP (3-fold) protein levels in total cell extracts from *bul1*Δ *bul2*Δ *pep4*Δ cells compared with *bul1*Δ *bul2*Δ cells. These differences in protein levels are stronger than the differences observed between *bul1*Δ *bul2*Δ and wild-type (Figure 3A), and between *pep4*Δ and wild-type (Figure 1D), suggesting that vacuolar degradation is a key player in the low protein levels observed in *bul1*Δ *bul2*Δ. Consistent with this hypothesis, the fluorescence signal of Ptr2-YFP in the *bul1*Δ *bul2*Δ strain was localized in the vacuole as well as in the plasma membrane (Figure 4C).

The deletion of Bul adaptors has no effect on Put4-9myc and Dal5 protein levels when Gap1 is missing

As Bul1 and Bul2 regulate the endocytosis of the general amino acid permease Gap1, we can imagine that the effect of Bul absence on Put4, Dal5 and Ptr2 protein levels could actually result from Gap1 stabilization at the plasma membrane. To test whether the low Put4-9myc and Dal5 protein levels in *bul1*Δ *bul2*Δ depends on Gap1 or not, we used a strain deleted for Bul1, Bul2 and the general amino acid permease Gap1 (*bul1*Δ *bul2*Δ *gap1*Δ), and quantified relative protein levels by Western blot (Figure 5). We found no significant difference in Put4-9myc and Dal5 protein levels between *gap1*Δ and *bul1*Δ *bul2*Δ *gap1*Δ strains. Accordingly, we found higher levels of Put4-9myc and Dal5 in *bul1*Δ *bul2*Δ *gap1*Δ than in *bul1*Δ *bul2*Δ, suggesting that Gap1 stabilization in the absence of Bul proteins is responsible for the low Put4, Dal5, and perhaps Ptr2, protein levels. To further test this hypothesis, we expressed Bul1-FLAG in *bul1*Δ *bul2*Δ *gap1*Δ, and observed no significant increase in Put4-9myc and Dal5 protein levels, confirming that the presence/absence of Bul proteins has no effect on Put4 and Dal5 protein levels when Gap1 is missing.

DISCUSSION

Yeast cells have evolved the ability to use a wide variety of nitrogen sources as the unique source of all the cellular nitrogen. According to the quality of the nitrogen source available, yeast cells modulate their set of nitrogen transporters present at the plasma membrane. This remodeling process involves both regulation of gene expression and post-translational regulation mechanisms. Transcriptomic studies identified genes that are up- or down-regulated in the presence of specific nitrogen sources, revealing for instance that many genes encoding transporters of non-preferred nitrogen sources are down-regulated when cells are supplied with a preferred nitrogen source. About post-translational regulation, previous reports have shown that the addition of a preferred nitrogen source to proline-grown cells triggers the Rsp5-Bul1/2-dependent ubiquitylation, endocytosis and vacuolar degradation of the general amino acid permease Gap1. However, there is a lack of knowledge about the post-translational regulation of other plasma membrane proteins, and this is what we addressed in the present study. Here, we used mass spectrometry-based proteomics to follow the dynamics of the plasma membrane proteome after the addition of a preferred nitrogen source to proline-grown cells. We identified (1) new targets of the nitrogen regulation, (2) four transporters of poor nitrogen sources—Put4, Opt2, Dal5 and Ptr2—that rapidly decrease in abundance. Although the kinetics is different for each transporter, we found that three of them—Put4, Dal5 and Ptr2— are endocytosed, like Gap1, in an Rsp5-dependent manner and degraded in the vacuole. (3) Finally, we showed that Gap1 stabilization at the plasma membrane, through deletion of Bul proteins, regulates the abundance of Put4, Dal5 and Ptr2. A model summarizing the trafficking of Gap1, Put4, Dal5 and Ptr2 in wild-type and mutant cells is presented in Figure 6.

To identify proteins that are differentially abundant in ammonium-grown cells vs. proline-grown cells, we used iTRAQ-based quantitative mass spectrometry. Protein identification and quantitation was performed separately for each biological replicate by the ProteinPilot software (Table S5). For each protein in each

biological replicate, ProteinPilot calculates an average ratio and a p-value assessing whether the protein can be considered as differentially abundant in the two conditions. Importantly, this p-value takes into account the number of peptide ratios used in the calculation of a protein ratio, hence rewarding proteins identified with more peptides, whose quantitation is considered as more reliable. To determine which proteins are differentially abundant in the two conditions, we combined data from the four biological replicates into a single p-value per protein and corrected this p-value for multiple testing. When a common hypothesis is tested in different samples taken from similar populations, an ideal approach is to pool raw data from all samples and conduct a single statistical test. When raw data cannot be pooled across samples, downstream statistical analysis (*t*-test, ANOVA) can be performed using the protein ratios. However, using only protein ratios for downstream statistical analysis presents one major limitation: it does not take into account the quality of the ratio. Ratios derived from a high number of high confidence peptides or from a unique peptide would be equally considered in the analysis, therefore rewarding protein ratios having low variability rather than high confidence. To tackle this limitation, Pascovici and colleagues proposed to use meta-analysis to combine p-values coming from different iTRAQ runs (30). In their paper, the authors describe a method known as "Stouffer's combined z-score" and propose to add a ratio trend consistency measurement to avoid rewarding proteins having low p-values but opposite direction of change. In the present study, we applied a meta-analysis based on weighted z-scores that takes into account the direction of change, and compared it with the p-value obtained after pooling peptides from the different biological replicates. This method has been first described by Liptak, and compared to other meta-analyses by Whitlock and Zaykin (25-27). In their studies, both Whitlock and Zaykin suggested that weighting is an important part of a meta-analysis as different studies might be differently powered. It is especially true in the context of iTRAQ ratios where similar ratios can come from a high number of high confidence peptides or from a unique peptide. Here, we used the square root of the sample size as a weight, i.e. the square root of the number of peptides that were used to compute a

protein ratio. Our comparison revealed that p-values obtained by combination of weighted z-scores are highly comparable to p-values obtained after pooling peptides from the four biological replicates, with a correlation coefficient reaching 99% after removal of the three lowest p-values that were reported as 0.0000 by ProteinPilot in all biological replicates (Figure S3B and Table S5). Such high correlation was not obtained using unweighted z-scores (data not shown).

In conclusion, our statistical analysis suggests that combination of p-values using weighted z-scores is a method of choice for downstream statistical analysis of iTRAQ ratios when peptide ratios cannot be pooled across iTRAQ runs.

New targets of the nitrogen regulation

Our proteomic screening revealed 27 plasma membrane proteins that vary in abundance between cells grown overnight either in proline- or ammonium-containing medium (Table 1). Most of them are described NCR targets, such as the transporters of nitrogenous compounds Gap1, Put4, Opt2, Dal5, Ptr2, Mep2 and Dur3 (5-7), the plasma membrane H^+-ATPase Pma1, the GTP-binding protein Ras2 involved in the regulation of sporulation, filamentous growth, and nitrogen starvation response, the GTPase Gpa2, which is required for the recruitment of Ras2 at the plasma membrane, and the GTPase Rho3 (33-35). Besides NCR targets, we identified other transporters known to be differentially expressed according to the nitrogen source, such as the multidrug transporter Qdr3, which was more abundant in proline-grown cultures. This transporter confers resistance to several drugs and polyamines (36, 37). *QDR3* transcript levels are up-regulated in yeast cells exposed to spermine and spermidine, and under nitrogen or amino acid limitation (37). This regulation is dependent on the transcription factor Gcn4, which controls amino acid biosynthesis. During growth on a poor nitrogen source, upregulation of *QDR3* expression might be necessary to export from the cells toxic polyamines that are uptaken together with urea and amino acids

by Dur3 and Gap1, respectively (38). From the screening, we also identified the histidine and methionine transporters Hip1 and Mup1. Unlike NCR-sensitive permeases that transport amino acids primarily for use as a source of nitrogen, Hip1 and Mup1 are though to transport specific amino acids for direct use in protein synthesis when the nitrogen conditions are favorable (39). *HIP1* and *MUP1* expression is induced by the SPS amino acid-sensing system and has been shown to be down-regulated in the presence of a poor nitrogen source, and this down-regulation requires the presence of Gap1 at the plasma membrane (5).

Interestingly, our screening revealed proteins that have never been described previously as targets of the nitrogen regulation, such as the glucose transporter Hxt4 and the ABC transporter Pdr5, both less abundant in proline-grown cultures, the protein kinase Yck2, which is involved in plasma membrane protein ubiquitylation and endocytosis, the t-SNARE Sso2 involved in the late secretory pathway, three proteins involved in cell wall synthesis (Gas3, Gas5 and Gsc2), a protein involved in lipid metabolism (Plb1), a protein of unknown function (Ecm33), and five major components of membrane compartments of Can1 (MCCs) and eisosomes (Pil1, Lsp1, Sur7, Ycp4 and Nce102), the latter ten being more abundant in proline-grown cultures. MCCs/eisosomes are specialized plasma membrane microdomains containing specific proteins. Although the formation and organization of eisosomes have already been described (40), their cellular function remains elusive. Previous studies suggested a role in endocytosis, but this remains a matter of debate (41, 42). Further investigation would be required to determine whether eisosomes and microdomains play a role in the nitrogen-induced regulation of plasma membrane proteins.

The identification of proteins that were known to be differentially expressed according to the nitrogen source gave us confidence that the method we used was valid, and that the proteins identified for the first time in this screening are actual targets of the nitrogen regulation. However, this screening in not exhaustive. For instance, we expected to identify more SPS-sensitive amino acid transporters, such as Tat2, Bap2 and Gnp1 (5). Another example is the proline transporter Put4 that we identified based on two peptides only. Although these two peptides were strongly more abundant in proline-grown cells, there

were not enough of them to allow reliable quantification. As Put4 is a known NCR target, we used Western blotting to confirm its abundance variation. In conclusion, although this technique enabled the detection and quantification of many proteins, including new targets of the nitrogen regulation, there likely remains interesting targets to discover.

Different kinetics of regulation for different transporters

As the variations in protein amounts observed in the steady-state mass-spectrometry experiment could reflect transcriptional, translational, as well as post-translational regulation, we analyzed the temporal evolution (up to 90 minutes) of the plasma membrane proteome of proline-grown yeast cells upon the addition of 10 mM ammonium. We observed that five different plasma membrane transporters decrease in abundance within the 90 minutes time window, following different kinetics (Figure 1A). Gap1, Put4 and Opt2 were the first proteins to decrease, followed by Dal5, and then Ptr2. These kinetics were confirmed by western blotting on total cell extracts (Figure 1B), suggesting protein degradation. All five proteins are known NCR targets, meaning that their expression is abolished upon the addition of a preferred nitrogen source. Therefore, a dilution effect due to cell division cannot be excluded, at least for proteins decreasing slowly in abundance (Dal5 and Ptr2). However, after the addition of a preferred nitrogen source to proline-grown cells, we observed the appearance of Gap1-GFP and Ptr2-YFP fluorescent dots inside the cells and a progressive staining of the vacuole (Figure 1C), suggesting endocytosis and vacuolar degradation. Nonetheless, as Ptr2-YFP was expressed under the control of the *GAP1* promoter, we cannot exclude artifacts due to overexpression, such as toxicity or mislocalization. Therefore, we used a strain deleted for the vacuolar protease Pep4 to verify the hypothesis of vacuolar degradation and observed that Pep4 deletion abolished the decrease in Gap1, Put4-9myc, Dal5, and Ptr2-YFP protein amounts in total cell extracts (Figure 1D). Finally, we showed that this decrease required functional Rsp5 ubiquitin ligase (Figure

2). Taken together, these results suggest that proteins decreasing in abundance within the 90 minutes time window undergo endocytosis and vacuolar degradation.

To summarize, we found that, like the amino acid transporter Gap1, the transporters of poor nitrogen sources Put4, Dal5 and Ptr2 are endocytosed and degraded upon the addition of a preferred nitrogen source to proline-grown cells. Previous studies have shown that Put4 and Dal5 are inactivated for their transport activity in an Rsp5-dependent manner upon the addition of a preferred nitrogen source to proline-grown cultures (10). Here, we confirmed that Put4 and Dal5, as well as Ptr2, are endocytosed in an Rsp5 ubiquitin ligase-dependent manner. However, contrary to Gap1, the endocytosis of Put4, Dal5 and Ptr2 does not require functional Bul1 and Bul2 ubiquitin ligase adaptors. In our attempts to identify the ubiquitin ligase adaptors involved in Put4 and Dal5 nitrogen-induced endocytosis, we observed that the *bul1*Δ *bul2*Δ, *9-arrestin*Δ, and *9-arrestin*Δ *bul1*Δ mutant strains were still able to degrade Put4 and Dal5. This suggests either (1) a direct interaction between the nitrogen transporters and the ubiquitin ligase Rsp5—which seems unlikely regarding the absence of PY motif in their sequence—or (2) another combination of ubiquitin ligase adaptors involving for instance Bul2 and other ARTs. Such a combination has been identified for the stress-induced endocytosis of Gap1 that can be mediated by Bul1, Bul2, Aly1/Art6 or Aly2/Art3 (43). Recently, Kawai and colleagues (44) documented that the addition of cycloheximide to cells grown in synthetic dextrose (SD) medium triggers Rsp5-dependent ubiquitylation and endocytosis of Ptr2. Cycloheximide induces TORC1-dependent endocytosis of many plasma membrane transporters (32, 45, 46). The nitrogen-induced internalization of Gap1 has been shown to be under the control of TORC1 as well (15). Accordingly, it seems very likely that a common mechanism triggering nitrogen- and cycloheximide-dependent endocytosis of a transporter exists. Consistent with this hypothesis, we found the same kinetics of protein signal disappearance for Gap1, Put4-9myc, Opt2 and Ptr2-9myc after the addition of ammonium or cycloheximide to proline-grown cultures (data not shown). In their study on Ptr2, Kawai *et al.* (44) identified Bul1 and Bul2 as the ubiquitin ligase adaptors mediating

Ptr2 cycloheximide-induced endocytosis. In the present study, we showed that Ptr2 is efficiently degraded upon addition of a preferred nitrogen source to proline-grown *bul1*Δ *bul2*Δ cells, suggesting that different combinations of adaptors might mediate nitrogen-dependent and cycloheximide-dependent endocytosis of transporters.

Why different kinetics of degradation exist for different transporters remains unanswered. Likewise, we were surprised to observe that five NCR-sensitive amino acid and peptide transporters were endocytosed upon the addition of a preferred nitrogen source, whereas the ammonium transporter Mep2 remained stable. The discovery of a novel TORC1-Npr1-dependent mechanism that tunes the inherent activity of Mep2 (47) could explain why Mep2 is not degraded within the 90 minutes time window. In this mechanism, which is independent of ART-mediated endocytosis, Npr1 activates Mep2 by catalyzing the silencing phosphorylation of a C-terminal autoinhibitory domain in the protein. This domain is rapidly dephosphorylated upon addition of a preferred source, leading to the inactivation of the permease. Mep1 and Mep3 were also shown to be inactivated in the presence of a preferred nitrogen source through interaction with the inhibitory protein Amu1, which is itself inhibited by Npr1 in poor nitrogen conditions (48). Future studies are necessary to determine whether other nitrogen transporters are subjected to such an inactivation process, and what are the molecular mechanisms determining which transporters are degraded, and how fast, and which others remain stable in an inactivated form at the plasma membrane.

Gap1 stabilization at the plasma membrane, through deletion of Bul proteins, regulates the abundance of Put4, Dal5 and Ptr2

While Bul proteins are not required for Put4, Dal5 and Ptr2 endocytosis, their deletion resulted in a dramatic decrease in Put4, Dal5 and Ptr2 total protein amounts. To discriminate between an effect of Bul deletion on gene transcription or on protein degradation, we measured the mRNA levels of *PUT4*, *DAL5* and *GAP1* in wild-type and *bul1*Δ *bul2*Δ strains and their protein levels in *bul1*Δ *bul2*Δ and *bul1*Δ *bul2*Δ

*pep4*Δ strains. Using q-RT-PCR, we observed a general 2-fold decrease of *PUT4*, *DAL5* and *GAP1* gene expression in the *bul1*Δ *bul2*Δ strain compared to wild-type, which was not sufficient to explain the 5-fold decrease observed at the protein level. In addition to this transcriptional regulation, we observed an 8-fold decrease in Put4-9myc and Dal5 protein levels in the *bul1*Δ *bul2*Δ strain compared to *bul1*Δ *bul2*Δ *pep4*Δ (Figure 4B), and a vacuolar and plasma membrane localization of Ptr2-YFP in *bul1*Δ *bul2*Δ, strongly suggesting vacuolar degradation. Taken together, these results indicate that both gene expression and protein stability were affected by the deletion of Bul proteins.

As the deletion of Bul proteins causes Gap1 stabilization at the plasma membrane, we determined whether the effect of Bul deletion on Put4 and Dal5 was dependent on Gap1. Interestingly, our results showed that, in a *gap1*Δ strain, the deletion of Bul1 and Bul2 had no effect on Put4 and Dal5 protein levels. This confirms that the lack of Gap1 endocytosis in the absence of Bul proteins is responsible for the low Put4 and Dal5 protein levels. Several hypotheses may be considered to explain this cross-regulation between Gap1 and other transporters of poor nitrogen sources. The first one is a modification of the intracellular pool of nitrogen. The stabilization of Gap1 at the plasma membrane might result in a better nitrogen assimilation leading to NCR and degradation of plasma membrane-localized transporters of poor nitrogen sources. This hypothesis is supported by our q-RT-PCR results, as all NCR genes tested—including Gap1—were down-regulated in the *bul1*Δ *bul2*Δ strain. In addition, we observed a 3-fold decrease of Put4-9myc and Dal5 protein levels in the *npi1* yeast strain, which is deficient for Rsp5 (Figure 2A). In this strain, Gap1 is also stabilized at the plasma membrane, which could in turn lead to NCR and protein degradation, except that plasma membrane-localized Put4 and Dal5 cannot be degraded in the absence of Rsp5, likely explaining why the decrease in protein amounts was less dramatic in *npi1* than in *bul1*Δ *bul2*Δ. Future studies are required to determine whether Gap1-dependent down-regulation of transporters of poor nitrogen sources is caused by improved nitrogen uptake. Experimentally, the total intracellular pools of amino acids in wild-type and *bul1*Δ *bul2*Δ cells could be compared as described in (49). Note that, in proline-growing

cells, Gap1 is already highly active and stable at the plasma membrane. Therefore, an improved nitrogen uptake in the absence of Bul proteins might seem unlikely. Alternatively, we could consider another explanation for the low Put4, Dal5 and Ptr2 protein levels. In a recent study on substrate-induced Gap1 endocytosis, Van Zeebroeck and colleagues showed that the addition of L-citrulline to nitrogen-starved cells expressing wild-type Gap1 and a mutant form of Gap1 deficient for transport activity ($Gap1^{Y395C}$) triggered the endocytosis of both wild-type Gap1 and $Gap1^{Y395C}$ (50). Endocytosis of $Gap1^{Y395C}$ was also observed when co-expressed with $Gap1^{K9R,K16R}$, which is itself deficient for endocytosis. On the contrary, $Gap1^{Y395C}$ expressed alone was not endocytosed upon the addition of L-citrulline. Taken together, their results suggest that an active Gap1 transporter can trigger the endocytosis "in trans" of an inactive transporter, even when the active transporter itself cannot be endocytosed. Based on these findings, we can imagine that an active Gap1 can also induce the endocytosis of other plasma membrane-localized nitrogen transporters. The authors proposed that, in the substrate-induced endocytosis of Gap1, the hyperphosphorylation of Npr1, leading to the release of Bul proteins from the 14-3-3 complex, may be triggered by a signal originating from the active Gap1 itself. As the stability of Put4 and Dal5 requires functional Npr1 kinase (51, 52), a similar mechanism involving other ubiquitin ligase adaptors than the Bul proteins, might provide a credible explanation to the low Put4, Dal5 and Ptr2 protein levels. Accordingly, we could hypothesize that a signal originating from Gap1 may be more persistent when Gap1 is sequestered at the plasma membrane in *bul1*Δ *bul2*Δ cells, hence triggering Put4, Dal5 and Ptr2 endocytosis.

Conclusion

In this study, we showed that mass spectrometry is a technique of choice to monitor the nitrogen-induced remodeling of the plasma membrane proteome and to approach the study of endocytic mechanisms. In addition to the known NCR-sensitive genes, we identified new targets of the nitrogen regulation, such as

members of eisosomes and MCCs. Using mass spectrometry, we followed the evolution over time of the plasma membrane proteome and found a group of nitrogen transporters that are rapidly endocytosed and degraded in the vacuole upon the addition of a preferred nitrogen source to proline-grown cells. Among them, the well-studied amino acid transporter Gap1, the proline permease Put4, the allantoate permease Dal5, and the peptide transporter Ptr2 (Figure 6A). While Rsp5 is required for the internalization of the four of them (Figure 6B), Bul adaptor proteins are only required for Gap1 endocytosis (Figure 6C). Remarkably, we found that the stabilization of Gap1 at the plasma membrane increases the vacuolar trafficking and degradation of the three other nitrogen transporters (Figure 6D). We believe this finding opens up new areas of investigation towards a thorough understanding of the regulation, and possibly cross-regulation, of plasma membrane transporters.

ACKNOWLEDGEMENTS

The authors thank Peter Kötter, Bruno André, Hugh Pelham, Cédric Govaerts, Michel Ghislain, Charles Barlowe, Howard Riezman, André Goffeau, Anna Maria Marini, Jan Malinsky, and Agustina Olivera-Couto for providing strains, plasmids and antibodies. We thank Bruno André and Sébastien Léon for constructive discussions and advice, and Henri-François Renard for critical reading of the paper. This work was supported by grants from the Fonds National de la Recherche Scientifique (FNRS) and the Fédération Wallonie-Bruxelles (ARC). J.V., J.S., A.S. and S.N. are research fellows at the “Fonds pour la formation à la Recherche dans l’Industrie et dans l’Agriculture".

1. Cooper TG. Nitrogen metabolism in *Saccharomyces cerevisiae*. In: Strathern JN, Jones EW, Broach JR, editors. The Molecular Biology of the Yeast *Saccharomyces*: Metabolism and Gene Expression. Cold Spring Harbor, NY: Cold Spring Harbor Laboratory Press; 1982. p. 39-99.
2. Jones EW, Fink GR. Regulation of amino acid and nucleotide biosynthesis in yeast. *Cold Spring Harbor Monograph Archive*; 1982. p. 181-299.
3. Magasanik B. Regulation of nitrogen utilization. In: Strathern JN, Jones EW, Broach JR, editors. The Molecular Biology of the Yeast *Saccharomyces cerevisiae*: Metabolism and Gene Expression. Cold Spring Harbor, NY: Cold Spring Harbor Laboratory Press; 1992. p. 283-317.
4. Magasanik B, Kaiser CA. Nitrogen regulation in Saccharomyces cerevisiae. Gene. 2002;290(1-2):1-18.
5. Scherens B, Feller A, Vierendeels F, Messenguy F, Dubois E. Identification of direct and indirect targets of the Gln3 and Gat1 activators by transcriptional profiling in response to nitrogen availability in the short and long term. FEMS Yeast Res. 2006;6(5):777-91.
6. Boer VM, Tai SL, Vuralhan Z, Arifin Y, Walsh MC, Piper MD, et al. Transcriptional responses of Saccharomyces cerevisiae to preferred and nonpreferred nitrogen sources in glucose-limited chemostat cultures. FEMS Yeast Res. 2007;7(4):604-20.
7. Godard P, Urrestarazu A, Vissers S, Kontos K, Bontempi G, van Helden J, et al. Effect of 21 different nitrogen sources on global gene expression in the yeast Saccharomyces cerevisiae. Mol Cell Biol. 2007;27(8):3065-86.
8. Airoldi EM, Miller D, Athanasiadou R, Brandt N, Abdul-Rahman F, Neymotin B, et al. Steady-state and dynamic gene expression programs in Saccharomyces cerevisiae in response to variation in environmental nitrogen. Mol Biol Cell. 2016;27(8):1383-96.
9. Gygi SP, Rochon Y, Franza BR, Aebersold R. Correlation between protein and mRNA abundance in yeast. Mol Cell Biol. 1999;19(3):1720-30.
10. Grenson M. Inactivation-reactivation process and repression of permease formation regulate several ammonia-sensitive permeases in the yeast Saccharomyces cerevisiae. Eur J Biochem. 1983;133(1):135-9.
11. Hein C, Springael JY, Volland C, Haguenauer-Tsapis R, André B. NPl1, an essential yeast gene involved in induced degradation of Gap1 and Fur4 permeases, encodes the Rsp5 ubiquitin-protein ligase. Mol Microbiol. 1995;18(1):77-87.
12. Springael JY, Galan JM, Haguenauer-Tsapis R, André B. NH4+-induced down-regulation of the Saccharomyces cerevisiae Gap1p permease involves its ubiquitination with lysine-63-linked chains. J Cell Sci. 1999;112 (Pt 9):1375-83.
13. Soetens O, De Craene JO, Andre B. Ubiquitin is required for sorting to the vacuole of the yeast general amino acid permease, Gap1. J Biol Chem. 2001;276(47):43949-57.
14. De Craene JO, Soetens O, Andre B. The Npr1 kinase controls biosynthetic and endocytic sorting of the yeast Gap1 permease. J Biol Chem. 2001;276(47):43939-48.
15. Merhi A, André B. Internal amino acids promote Gap1 permease ubiquitylation via TORC1/Npr1/14-3-3-dependent control of the Bul arrestin-like adaptors. Mol Cell Biol. 2012;32(22):4510-22.
16. Springael JY, André B. Nitrogen-regulated ubiquitination of the Gap1 permease of Saccharomyces cerevisiae. Mol Biol Cell. 1998;9(6):1253-63.
17. Helliwell SB, Losko S, Kaiser CA. Components of a ubiquitin ligase complex specify polyubiquitination and intracellular trafficking of the general amino acid permease. J Cell Biol. 2001;153(4):649-62.
18. Walther TC, Mann M. Mass spectrometry-based proteomics in cell biology. J Cell Biol. 2010;190(4):491-500.

19. Boisvert FM, Ahmad Y, Gierliński M, Charrière F, Lamont D, Scott M, et al. A quantitative spatial proteomics analysis of proteome turnover in human cells. Mol Cell Proteomics. 2012;11(3):M111.011429.
20. Debailleul F, Trubbia C, Frederickx N, Lauwers E, Merhi A, Ruysschaert JM, et al. Nitrogen catabolite repressible GAP1 promoter, a new tool for efficient recombinant protein production in S. cerevisiae. Microb Cell Fact. 2013;12:129.
21. Szopinska A, Degand H, Hochstenbach JF, Nader J, Morsomme P. Rapid response of the yeast plasma membrane proteome to salt stress. Mol Cell Proteomics. 2011;10(11):M111.009589.
22. Morsomme P, Chami M, Marco S, Nader J, Ketchum KA, Goffeau A, et al. Characterization of a hyperthermophilic P-type ATPase from Methanococcus jannaschii expressed in yeast. J Biol Chem. 2002;277(33):29608-16.
23. De Block J, Szopinska A, Guerriat B, Dodzian J, Villers J, Hochstenbach JF, et al. The yeast Pmp3p has a significant role in plasma membrane organization. J Cell Sci. 2015;128(19):1489-500.
24. Smith PK, Krohn RI, Hermanson GT, Mallia AK, Gartner FH, Provenzano MD, et al. Measurement of protein using bicinchoninic acid. Anal Biochem. 1985;150(1):76-85.
25. Liptak T. On the combination of independent tests. Magyar Tud Akad Mat Kutato Int Kozl. 1958;3:171-97.
26. Whitlock MC. Combining probability from independent tests: the weighted Z-method is superior to Fisher's approach. J Evol Biol. 2005;18(5):1368-73.
27. Zaykin DV. Optimally weighted Z-test is a powerful method for combining probabilities in meta-analysis. J Evol Biol. 2011;24(8):1836-41.
28. Pfaffl MW. A new mathematical model for relative quantification in real-time RT-PCR. Nucleic Acids Res. 2001;29(9):e45.
29. Brohée S, Barriot R, Moreau Y, André B. YTPdb: a wiki database of yeast membrane transporters. Biochim Biophys Acta. 2010;1798(10):1908-12.
30. Pascovici D, Song X, Solomon PS, Winterberg B, Mirzaei M, Goodchild A, et al. Combining protein ratio p-values as a pragmatic approach to the analysis of multirun iTRAQ experiments. J Proteome Res. 2015;14(2):738-46.
31. Jauniaux JC, Vandenbol M, Vissers S, Broman K, Grenson M. Nitrogen catabolite regulation of proline permease in Saccharomyces cerevisiae. Cloning of the PUT4 gene and study of PUT4 RNA levels in wild-type and mutant strains. Eur J Biochem. 1987;164(3):601-6.
32. Nikko E, Pelham HR. Arrestin-mediated endocytosis of yeast plasma membrane transporters. Traffic. 2009;10(12):1856-67.
33. Usaite R, Patil KR, Grotkjaer T, Nielsen J, Regenberg B. Global transcriptional and physiological responses of Saccharomyces cerevisiae to ammonium, L-alanine, or L-glutamine limitation. Appl Environ Microbiol. 2006;72(9):6194-203.
34. Cox KH, Pinchak AB, Cooper TG. Genome-wide transcriptional analysis in S. cerevisiae by mini-array membrane hybridization. Yeast. 1999;15(8):703-13.
35. MacIsaac KD, Wang T, Gordon DB, Gifford DK, Stormo GD, Fraenkel E. An improved map of conserved regulatory sites for Saccharomyces cerevisiae. BMC Bioinformatics. 2006;7:113.
36. Tenreiro S, Vargas RC, Teixeira MC, Magnani C, Sá-Correia I. The yeast multidrug transporter Qdr3 (Ybr043c): localization and role as a determinant of resistance to quinidine, barban, cisplatin, and bleomycin. Biochem Biophys Res Commun. 2005;327(3):952-9.
37. Teixeira MC, Cabrito TR, Hanif ZM, Vargas RC, Tenreiro S, Sá-Correia I. Yeast response and tolerance to polyamine toxicity involving the drug : H+ antiporter Qdr3 and the transcription factors Yap1 and Gcn4. Microbiology. 2011;157(Pt 4):945-56.
38. Uemura T, Kashiwagi K, Igarashi K. Polyamine uptake by DUR3 and SAM3 in Saccharomyces cerevisiae. J Biol Chem. 2007;282(10):7733-41.

39. Olivera H, González A, Peña A. Regulation of the amino acid permeases in nitrogen-limited continuous cultures of the yeast Saccharomyces cerevisiae. Yeast. 1993;9(10):1065-73.
40. Olivera-Couto A, Aguilar PS. Eisosomes and plasma membrane organization. Mol Genet Genomics. 2012;287(8):607-20.
41. Walther TC, Brickner JH, Aguilar PS, Bernales S, Pantoja C, Walter P. Eisosomes mark static sites of endocytosis. Nature. 2006;439(7079):998-1003.
42. Brach T, Specht T, Kaksonen M. Reassessment of the role of plasma membrane domains in the regulation of vesicular traffic in yeast. J Cell Sci. 2011;124(Pt 3):328-37.
43. Crapeau M, Merhi A, André B. Stress conditions promote yeast Gap1 permease ubiquitylation and down-regulation via the arrestin-like Bul and Aly proteins. J Biol Chem. 2014;289(32):22103-16.
44. Kawai K, Moriya A, Uemura S, Abe F. Functional implications and ubiquitin-dependent degradation of the peptide transporter Ptr2 in Saccharomyces cerevisiae. Eukaryot Cell. 2014;13(11):1380-92.
45. Lin CH, MacGurn JA, Chu T, Stefan CJ, Emr SD. Arrestin-related ubiquitin-ligase adaptors regulate endocytosis and protein turnover at the cell surface. Cell. 2008;135(4):714-25.
46. MacGurn JA, Hsu PC, Smolka MB, Emr SD. TORC1 regulates endocytosis via Npr1-mediated phosphoinhibition of a ubiquitin ligase adaptor. Cell. 2011;147(5):1104-17.
47. Boeckstaens M, Llinares E, Van Vooren P, Marini AM. The TORC1 effector kinase Npr1 fine tunes the inherent activity of the Mep2 ammonium transport protein. Nat Commun. 2014;5:3101.
48. Boeckstaens M, Merhi A, Llinares E, Van Vooren P, Springael JY, Wintjens R, et al. Identification of a Novel Regulatory Mechanism of Nutrient Transport Controlled by TORC1-Npr1-Amu1/Par32. PLoS Genet. 2015;11(7):e1005382.
49. Fayyad-Kazan M, Feller A, Bodo E, Boeckstaens M, Marini AM, Dubois E, et al. Yeast nitrogen catabolite repression is sustained by signals distinct from glutamine and glutamate reservoirs. Mol Microbiol. 2016;99(2):360-79.
50. Van Zeebroeck G, Rubio-Texeira M, Schothorst J, Thevelein JM. Specific analogues uncouple transport, signalling, oligo-ubiquitination and endocytosis in the yeast Gap1 amino acid transceptor. Mol Microbiol. 2014;93(2):213-33.
51. Grenson M. Study of the positive control of the general amino-acid permease and other ammonia-sensitive uptake systems by the product of the NPR1 gene in the yeast Saccharomyces cerevisiae. Eur J Biochem. 1983;133(1):141-4.
52. Vandenbol M, Jauniaux JC, Grenson M. The Saccharomyces cerevisiae NPR1 gene required for the activity of ammonia-sensitive amino acid permeases encodes a protein kinase homologue. Mol Gen Genet. 1990;222(2-3):393-9.
53. Nijkamp JF, van den Broek M, Datema E, de Kok S, Bosman L, Luttik MA, et al. De novo sequencing, assembly and analysis of the genome of the laboratory strain Saccharomyces cerevisiae CEN.PK113-7D, a model for modern industrial biotechnology. Microb Cell Fact. 2012;11:36.

FIGURE LEGENDS

Figure 1. Five plasma membrane proteins are endocytosed and degraded at different rates after the addition of a rich nitrogen source to proline-grown cultures.

(A) Wild-type yeast cells (CEN.PK background) grown in proline-containing medium were incubated with 10 mM ammonium ($+NH_4^+$) for 0 (before NH_4^+ addition), 15, 45 and 90 minutes. Plasma membrane enriched fractions were analyzed by LC-MS/MS using iTRAQ labeling and relative protein levels were quantified using the zero minute time point as a reference for each single condition. Line charts show for each protein of interest the average quantification of all the peptides from the three biological replicates. Stars indicate the number of biological replicates having a ratio significantly lower than 1 (p-value < 0.05). Raw MS data are presented in Tables S5 and S6. **(B)** Total extracts from cells grown as in **(A)** were analyzed by western blotting using antibodies raised against Gap1, myc tag (for Put4-9myc and Ptr2-9myc), Opt2, Dal5, and Nce102. Line charts show quantification of western blotting signals. The zero minute time point was used as a reference for each single condition. All biological replicates (their number being referred as n=X) are plotted on the charts and geometric means are connected by a line. Stars indicate when the ratio is significantly different from 1 with a p-value < 0.05 (*), < 0.01 (**), and < 0.001 (***). **(C)** Wild-type yeast cells (BY background) expressing Gap1-GFP, Ptr2-YFP, Qdr3-YFP, or Mep2-YFP (from a plasmid) were grown in proline-containing medium and incubated with 10 mM glutamine (+Gln) for 0 (before Gln addition), 15, 45 and 90 minutes. The trafficking of Gap1-GFP, Ptr2-YFP, Qdr3-YFP and Mep2-YFP was followed by fluorescence microscopy. **(D)** Total extracts from wild-type and *pep4*Δ yeast strains (BY background) grown as in **(C)** were analyzed by western blotting using antibodies raised against Gap1, myc tag (for Put4-9myc), Dal5, GFP (for Ptr2-YFP), and Nce102. Nce102 was used as a loading control. Line charts show quantification of western blotting signals. The zero minute time point was used as a reference for each single condition. All biological replicates (their number being referred as n=X) are plotted on the charts and geometric means are connected by a line. Stars indicate for each time point when the protein ratios in WT and in *pep4*Δ are significantly different from each other with a p-value < 0.05 (*), < 0.01 (**), and < 0.001 (***). Histograms show the ratios at time zero between the protein levels in *pep4*Δ and in WT ± standard error. The number of biological replicates is indicated on the graphs (n=X). Stars indicate when the protein ratios are significantly lower than 1 with a p-value < 0.05 (*), < 0.01 (**), and < 0.001 (***).

Figure 2. The degradation of Gap1, Put4-9myc, Dal5 and Ptr2-YFP requires the ubiquitin ligase Rsp5

Wild-type and *npi1* yeast strains (BY background) grown in proline-containing medium were incubated with 10 mM glutamine (+Gln) for 0, 15, 45 and 90 minutes. **(A)** Total cell extracts were analyzed by western blotting using antibodies raised against Gap1, myc tag (for Put4-9myc), Dal5, GFP (for Ptr2-YFP) and Nce102. Nce102 was used as a loading control. Line charts show quantification of western blotting signals. The zero minute time point was used as a reference for each single condition. All biological replicates (their number being referred as n=X) are plotted on the charts and geometric means are connected by a line. Stars indicate for each time point when the protein ratios in WT and in *npi1* are significantly different from each other with a p-value < 0.05 (*), < 0.01 (**), and < 0.001 (***). Histograms show the ratios at time zero between the protein levels in *npi1* and in WT ± standard error. The number of biological replicates is indicated on the graphs (n=X). Stars indicate when the protein ratios are significantly lower than 1 with a p-value < 0.05 (*), < 0.01 (**), and < 0.001 (***). **(B)** The trafficking of Ptr2-YFP was followed by fluorescence microscopy.

Figure 3. Loss of Bul1 and Bul2 function results in very low levels of Put4-9myc, Dal5 and Ptr2-YFP proteins

(A) Wild-type and *bul1Δ bul2Δ* yeast strains (BY background) grown in proline-containing medium were incubated with 10 mM glutamine (+Gln) for 0, 15, 45 and 90 minutes. Total cell extracts were analyzed by western blotting using antibodies raised against Gap1, myc tag (for Put4-9myc), Dal5, GFP (for Ptr2-YFP) and Nce102. Nce102 was used as a loading control. Line charts show quantification of western blotting signals. The zero minute time point was used as a reference for each single condition. All biological replicates (their number being referred as n=X) are plotted on the charts and geometric means are connected by a line. Stars indicate for each time point when the protein ratios in WT and in *bul1*Δ *bul2*Δ are significantly different from each other with a p-value < 0.05 (*), < 0.01 (**), and < 0.001 (***). Histograms show the ratios at time zero between the protein levels in *bul1*Δ *bul2*Δ and in WT ± standard error. The number of biological replicates is indicated on the graph (n=X). Stars indicate when the protein ratios are significantly lower than 1 with a p-value < 0.05 (*), < 0.01 (**), and < 0.001 (***). **(B)** Wild-type, *9-arrestin*Δ *bul1*Δ *bul2*Δ, *9-arrestin*Δ *bul1*Δ, *9-arrestin*Δ, *bul1*Δ, and *bul2*Δ yeast strains (BY background) grown as in **(A)** were analyzed

by western blotting using antibodies raised against Gap1, myc tag (for Put4-9myc), Dal5 and Nce102. Nce102 was used as a loading control. **(C)** *bul1*Δ *bul2*Δ yeast strain (BY background) was transformed with plasmids expressing wild-type Bul1, or the Bul1 mutant PPSY>AASY. The different transformants were grown as in **(A)** and analyzed by western blotting using antibodies raised against Gap1, myc tag (for Put4-9myc), Dal5, Nce102, and FLAG tag (for Bul1- and Bul1$^{PPSY>AASY}$-FLAG). Nce102 was used as a loading control. Histograms show the ratios at time zero between the protein levels in *bul1*Δ *bul2*Δ, *bul1*Δ *bul2*Δ + Bul1 and *bul1*Δ *bul2*Δ + Bul1$^{PPSY>AASY}$ ± standard error. The number of biological replicates is indicated on the graph (n=X). Stars indicate when the protein ratios are significantly lower than 1 with a p-value < 0.05 (*), < 0.01 (**), and < 0.001 (***).

Figure 4. Loss of Bul1 and Bul2 function results in vacuolar degradation of Put4-9myc, Dal5 and Ptr2-YFP

(A) Wild-type and *bul1*Δ *bul2*Δ yeast strains (BY background) were grown in proline-containing medium. Relative mRNA levels of *GAP1*, *PUT4* and *DAL5* were measured using quantitative real-time polymerase chain reaction (q-RT-PCR). *UBC6*, *TAF10* and *ALG9* were used as controls for stable gene expression. Histograms show the ratios between the mRNA levels in *bul1*Δ *bul2*Δ and in WT ± standard error (four biological replicates). Stars indicate when the mRNA ratio of a gene of interest is significantly different from the mRNA ratios of the control genes with a p-value < 0.05 (*), < 0.01 (**), and < 0.001 (***). **(B)** *bul1*Δ *bul2*Δ and *bul1*Δ *bul2*Δ *pep4*Δ yeast strains (BY background) grown in proline-containing medium were incubated with 10 mM glutamine (+Gln) for 0, 15, 45 and 90 minutes. Total cell extracts were analyzed by western blotting using antibodies raised against Gap1, myc tag (for Put4-9myc), Dal5, GFP (for Ptr2-YFP) and Nce102. Nce102 was used as a loading control. Histograms show the ratios at time zero between the protein levels in *bul1*Δ *bul2*Δ and in *bul1*Δ *bul2*Δ *pep4*Δ ± standard error. The number of biological replicates is indicated on the graph (n=X). Stars indicate when the protein ratios are significantly lower than 1 with a p-value < 0.05 (*), < 0.01 (**), and < 0.001 (***). **(C)** *bul1*Δ *bul2*Δ yeast cells (BY background) were grown as in **(B)** and the trafficking of Ptr2-YFP was followed by fluorescence microscopy.

Figure 5. The deletion of Bul adaptors has no effect on Put4-9myc and Dal5 protein levels when Gap1 is missing

*gap1*Δ, *bul1*Δ *bul2*Δ, *gap1*Δ *bul1*Δ *bul2*Δ, and *gap1*Δ *bul1*Δ *bul2*Δ complemented with wild-type Bul1 (BY background) grown in proline-containing medium were incubated with 10 mM glutamine (+Gln) for 0, 15, 45 and 90 minutes. Total cell extracts were analyzed by western blotting using antibodies raised against Gap1, myc tag (for Put4-9myc), Dal5, and Nce102. Nce102 was used as a loading control. Histograms show the ratios at time zero between the protein levels in *gap1*Δ, *bul1*Δ *bul2*Δ, *bul1*Δ *bul2*Δ *gap1*Δ, and *bul1*Δ *bul2*Δ *gap1*Δ + Bul1 ± standard error. The number of biological replicates is indicated on the graph (n=X). Stars indicate that the *bul1*Δ *bul2*Δ to *bul1*Δ *bul2*Δ *gap1*Δ protein ratios are significantly different from the other ratios with a p-value < 0.05 (*), < 0.01 (**), and < 0.001 (***).

Figure 6. Model summarizing the trafficking of Gap1, Put4, Dal5 and Ptr2 in wild-type and mutant strains

A. Gap1, Put4, Dal5 and Ptr2 are endocytosed and degraded in the vacuole upon the addition of a preferred nitrogen source (Glutamine) to proline-grown wild-type cells**. B.** Internalization of Gap1, Put4, Dal5 and Ptr2 is prevented in a strain deficient for the Rsp5 ubiquitin ligase. **C. *Left.*** In proline-grown cells deleted for the Bul1 and Bul2 ubiquitin ligase adaptors (*bul1*Δ *bul2*Δ), Put4, Dal5 and Ptr2 levels at the plasma membrane are strongly reduced compared with their protein levels in wild-type cells, and the proteins are targeted to the vacuole for degradation. ***Right.*** When a preferred nitrogen source is added to proline-grown *bul1*Δ *bul2*Δ cells, remaining plasma membrane-localized Put4, Dal5 and Ptr2 are endocytosed and degraded in the vacuole, while Gap1 remains stable at the plasma membrane. **D.** When Gap1 is deleted in addition to Bul1 and Bul2 (*bul1*Δ *bul2*Δ *gap1*Δ), Put4, Dal5 and Ptr2 are no longer degraded in the vacuole in proline-grown cells.

Table 1. The abundance of 27 plasma membrane proteins varies according to the nitrogen source

Wild-type yeast cells (CEN.PK background) were grown in liquid medium containing either proline or ammonium as unique nitrogen source and the plasma membrane proteome was quantitatively compared using iTRAQ. A total of 117 plasma membrane proteins were identified in this experiment (see Tables S5 and S6 for raw MS data). Table 1 shows proteins that vary in abundance between the two growth conditions with a cutoff level of significance of 95% (or p-value < 0.05) after Bonferroni correction. Quantitative results are expressed as ratios (ammonium-grown cells / proline-grown cells). Two different methods were used to calculate ratios and p-values. The first method is a single statistical analysis based on pooled peptide ratios from all biological replicates. The second method is a meta-analysis combining ratios and p-values from the different biological replicates. Both results are presented in Table 1.

Accession number	Name	Description	Pooled peptides		Meta-analysis	
			Average ratio	p-value	Average ratio	p-value
Transporters of nitrogenous compounds						
Q06593	Opt2	Oligopeptide transporter	0.025	2.8E-43	0.024	8.3E-15
P15365	Dal5	Allantoate-ureidosuccinate permease	0.018	1.5E-35	0.018	1.1E-14
P19145	Gap1	General amino acid permease	0.029	2.7E-33	0.029	8.2E-15
P41948	Mep2	Ammonium permease	0.106	5.3E-09	0.094	1.4E-08
P33413	Dur3	Urea and polyamine transporter	0.062	3.2E-07	0.050	4.3E-08
P06775	Hip1	Histidine permease	3.23	5.4E-05	2.69	4.6E-05
P32901	Ptr2	Peptide transporter	0.131	0.00015	0.160	0.00037
P50276	Mup1	Methionine permease	2.60	0.00019	2.18	0.00022
Other transporters						
P32467	Hxt4	Glucose transporter	4.43	8.0E-10	4.35	2.2E-08
P38227	Qdr3	Multidrug transporter	0.198	9.3E-06	0.233	3.7E-08
P33302	Pdr5	ABC transporter	1.82	4.3E-05	1.78	1.4E-06
Plasma membrane ATPase						
P05030	Pma1	Plasma membrane H^+-ATPase	0.263	5.8E-19	0.252	8.2E-15
Components of eisosomes and microdomains MCC						
P53252	Pil1	Primary component of eisosomes	0.358	9.7E-09	0.337	3.4E-08
Q12230	Lsp1	Primary component of eisosomes	0.293	4.0E-08	0.283	1.3E-06
Q12207	Nce102	MCC-localized protein	0.354	5.0E-06	0.351	1.2E-05
P54003	Sur7	Component of eisosomes	0.310	6.0E-05	0.305	7.1E-05
P25349	Ycp4	Protein of unknown function	0.547	0.00012	0.513	7.4E-05
Secretory pathway						
P39926	Sso2	Plasma membrane t-SNARE	0.497	3.7E-05	0.481	5.6E-05
Regulatory processes						
Q00245	Rho3	GTPase	0.441	1.7E-05	0.420	0.00023
P01120	Ras2	GTP-binding protein	0.532	5.8E-05	0.518	6.3E-07
P23292	Yck2	Casein kinase I	0.505	7.5E-05	0.480	0.00028
P10823	Gpa2	GTPase	0.568	0.0003	0.548	0.00018
Cell wall integrity						
Q08193	Gas5	1,3-beta-glucanosyltransferase	0.131	4.5E-11	0.125	2.8E-11
P40989	Gsc2	1,3-beta-glucan synthase	0.390	1.6E-07	0.377	3.1E-07
Q03655	Gas3	1,3-beta-glucanosyltransferase	0.486	5.5E-05	0.458	0.00012
Lipid metabolism						
P39105	Plb1	Phospholipase B	0.505	3.0E-05	0.480	3.6E-05
Unknown function						
P38248	Ecm33	GPI-anchored protein of unknown function	0.482	2.7E-05	0.476	8.5E-05

Figure 1

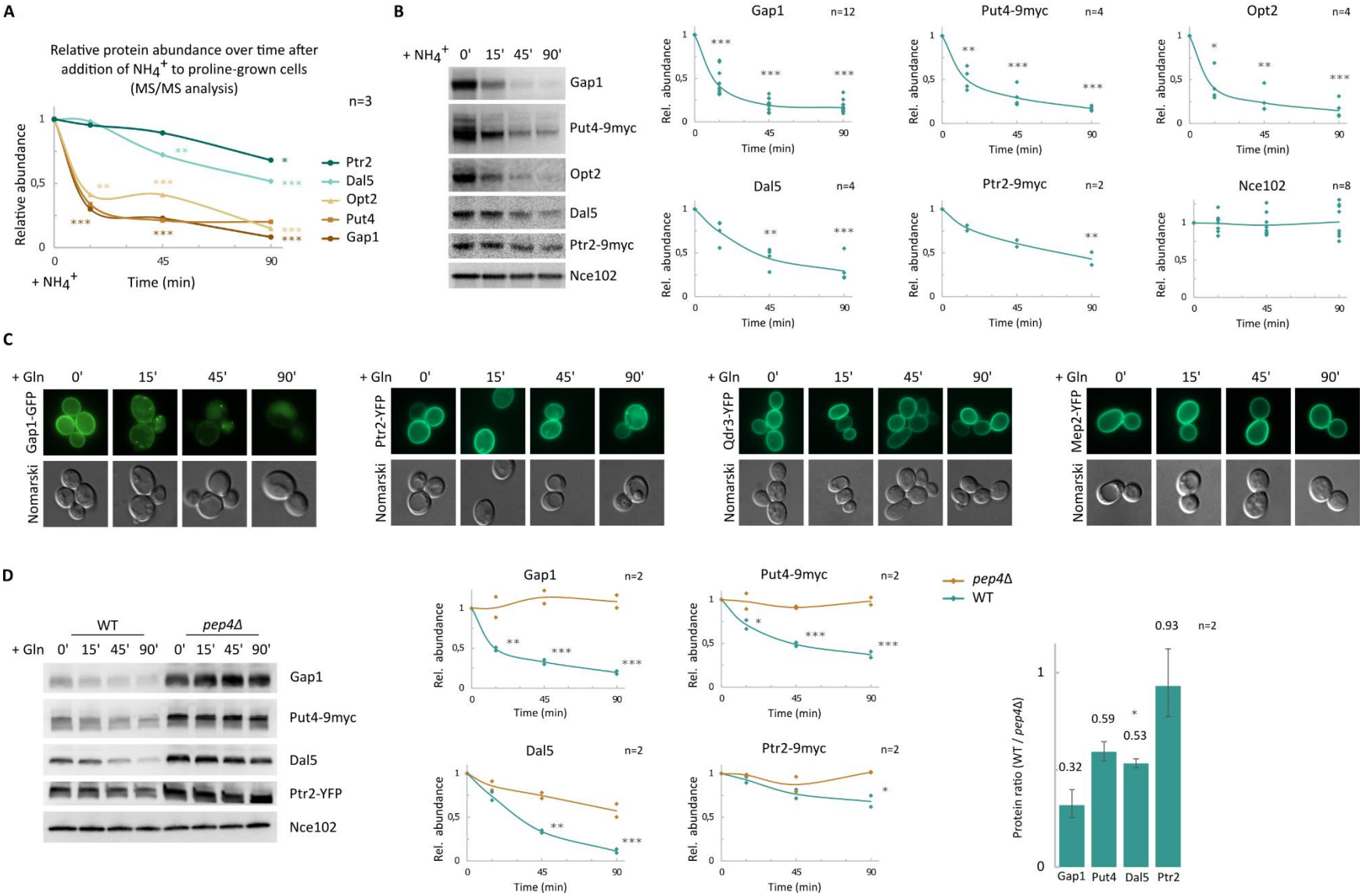
A
Relative protein abundance over time after addition of NH4+ to proline-grown cells (MS/MS analysis)
n=3
Relative abundance
Time (min)
+ NH4+
Ptr2
Dal5
Opt2
Put4
Gap1
B
+ NH4+ 0' 15' 45' 90'
Gap1
Put4-9myc
Opt2
Dal5
Ptr2-9myc
Nce102
Gap1 n=12
Put4-9myc n=4
Opt2 n=4
Dal5 n=4
Ptr2-9myc n=2
Nce102 n=8
Rel. abundance
Time (min)
C
+ Gln 0' 15' 45' 90'
Gap1-GFP
Ptr2-YFP
Qdr3-YFP
Mep2-YFP
Nomarski
D
WT
pep4Δ
+ Gln 0' 15' 45' 90' 0' 15' 45' 90'
Gap1
Put4-9myc
Dal5
Ptr2-YFP
Nce102
Gap1 n=2
Put4-9myc n=2
Dal5 n=2
Ptr2-9myc n=2
pep4Δ
WT
Rel. abundance
Time (min)
Protein ratio (WT / pep4Δ)
0.32
0.59
0.53
0.93
n=2
Gap1 Put4 Dal5 Ptr2

Figure 2

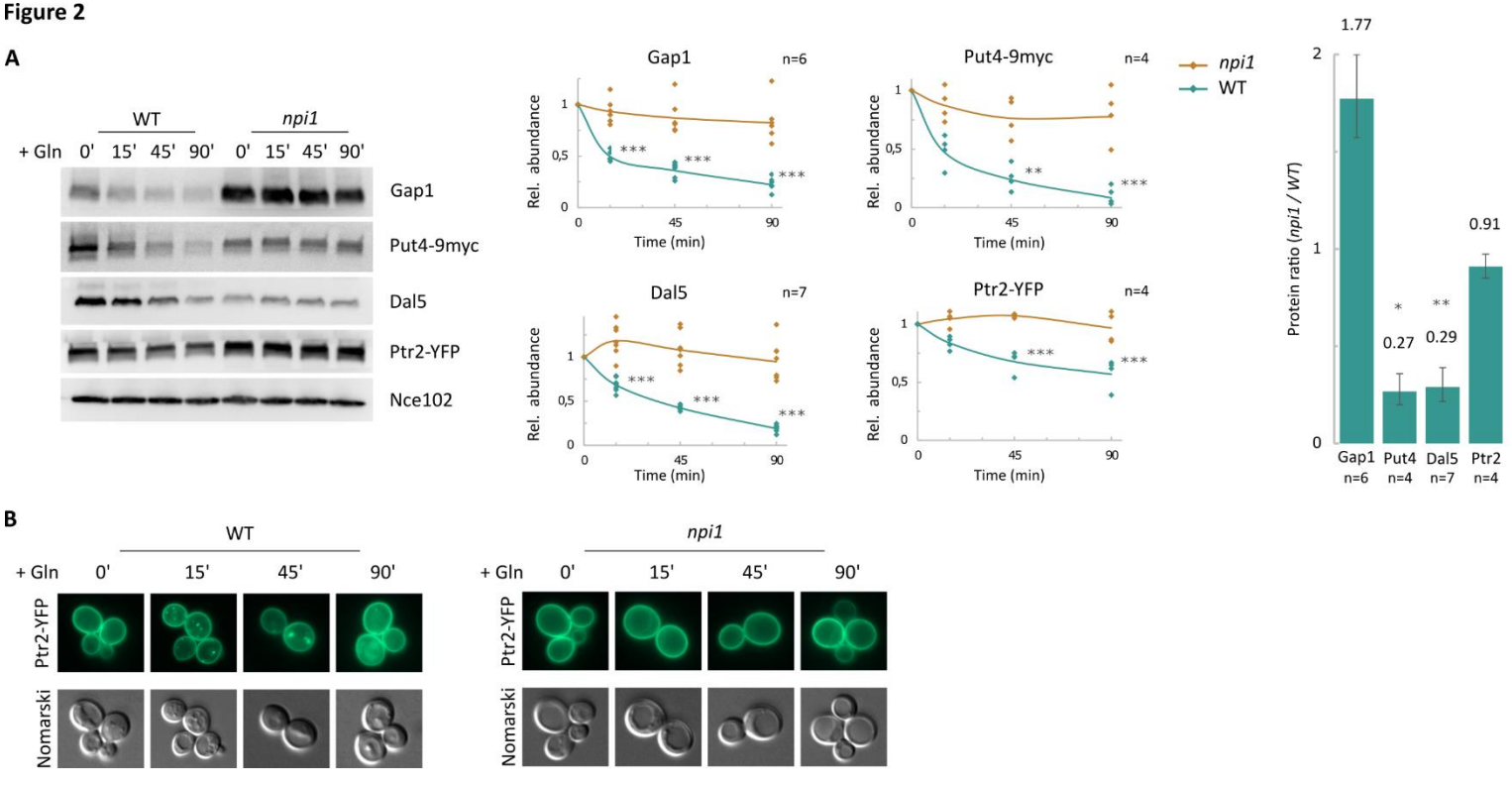
A
WT
npi1
+ Gln 0' 15' 45' 90' 0' 15' 45' 90'
Gap1
Put4-9myc
Dal5
Ptr2-YFP
Nce102
Gap1 n=6
Put4-9myc n=4
Dal5 n=7
Ptr2-YFP n=4
Rel. abundance
Time (min)
npi1
WT
Protein ratio (npi1 / WT)
1.77
0.27
0.29
0.91
Gap1 n=6
Put4 n=4
Dal5 n=7
Ptr2 n=4
B
WT
npi1
+ Gln 0' 15' 45' 90'
Ptr2-YFP
Nomarski

Figure 3

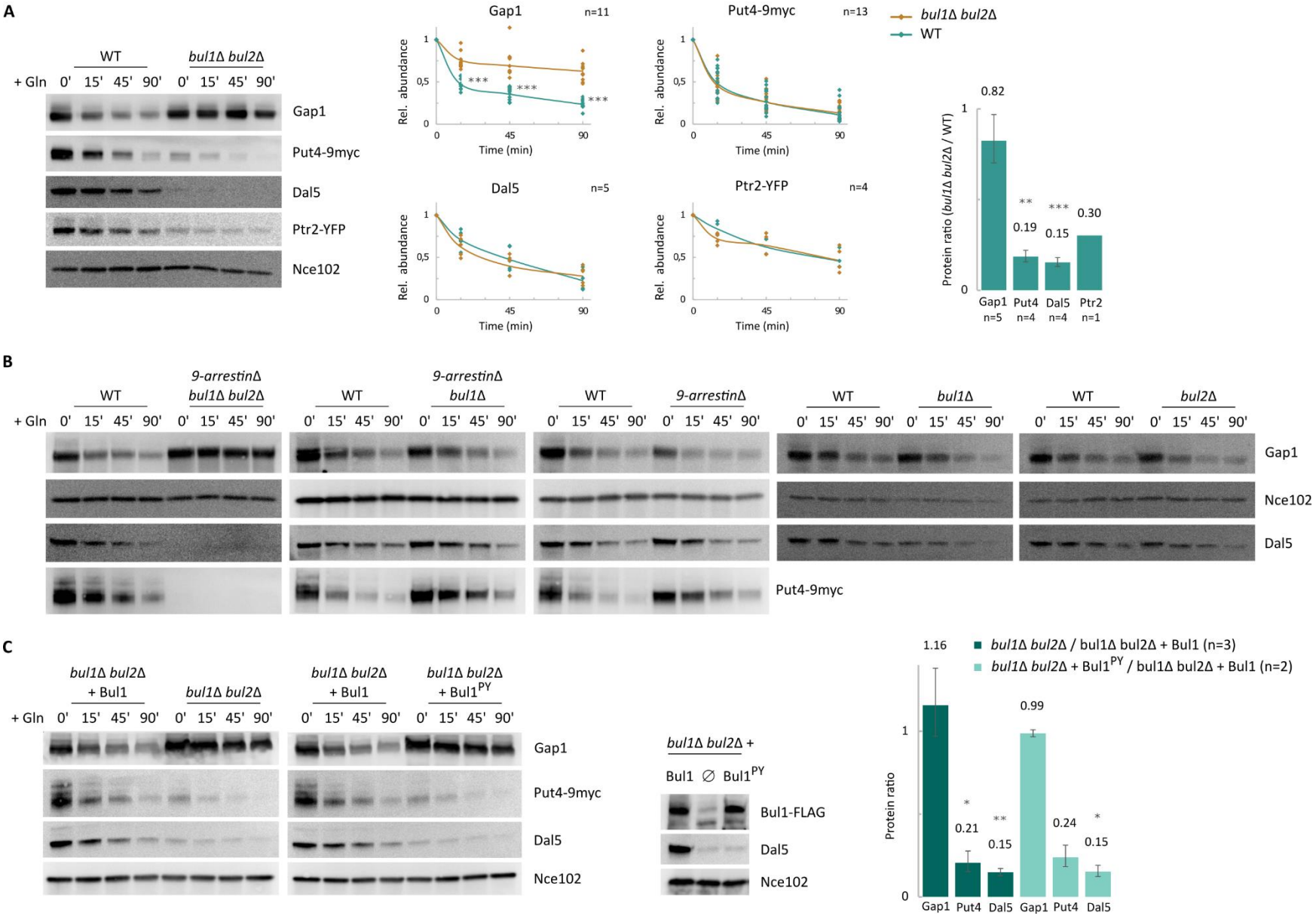
A
WT
bul1Δ bul2Δ
+ Gln 0' 15' 45' 90' 0' 15' 45' 90'
Gap1
Put4-9myc
Dal5
Ptr2-YFP
Nce102
Gap1 n=11
Put4-9myc n=13
Dal5 n=5
Ptr2-YFP n=4
Rel. abundance
Time (min)
bul1Δ bul2Δ
WT
Protein ratio (bul1Δ bul2Δ / WT)
0.82
0.19
0.15
0.30
Gap1 n=5
Put4 n=4
Dal5 n=4
Ptr2 n=1
B
9-arrestinΔ bul1Δ bul2Δ
9-arrestinΔ bul1Δ
9-arrestinΔ
bul1Δ
bul2Δ
C
bul1Δ bul2Δ + Bul1
bul1Δ bul2Δ + Bul1PY
bul1Δ bul2Δ +
Bul1 ∅ Bul1PY
Bul1-FLAG
bul1Δ bul2Δ / bul1Δ bul2Δ + Bul1 (n=3)
bul1Δ bul2Δ + Bul1PY / bul1Δ bul2Δ + Bul1 (n=2)
Protein ratio
1.16
0.21
0.15
0.99
0.24
0.15
Gap1 Put4 Dal5 Gap1 Put4 Dal5

Figure 4

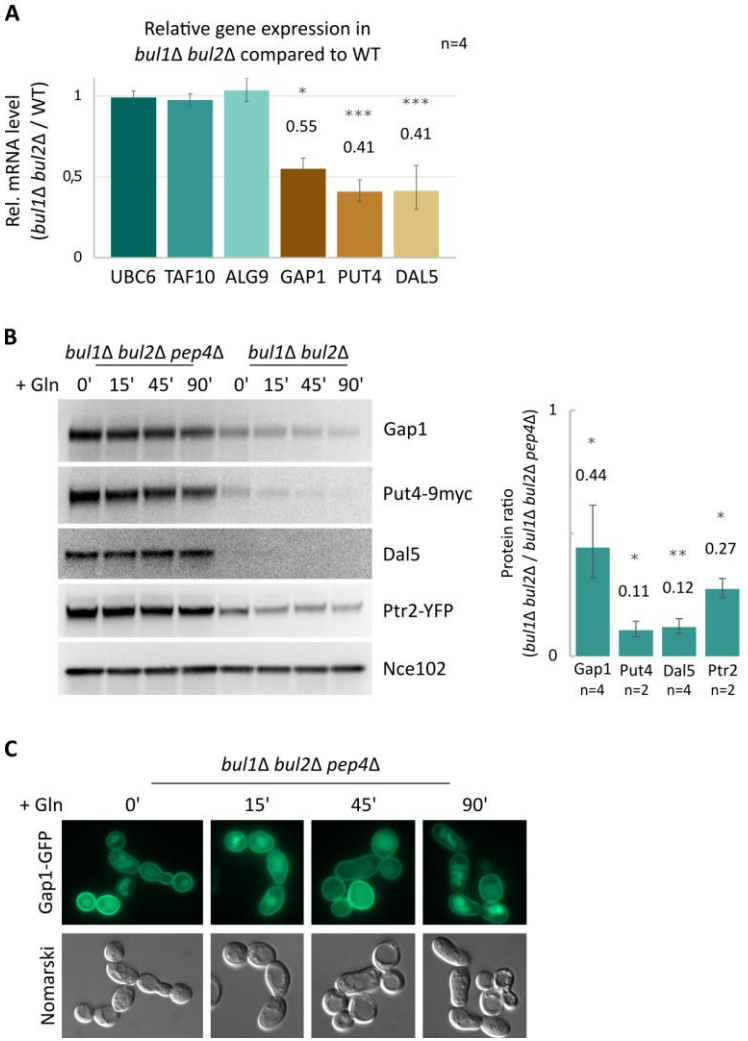
A
Relative gene expression in
bul1Δ bul2Δ compared to WT
n=4
Rel. mRNA level
(bul1Δ bul2Δ / WT)
1
0,5
0
*
***
***
0.55
0.41
0.41
UBC6 TAF10 ALG9 GAP1 PUT4 DAL5
B
bul1Δ bul2Δ pep4Δ
bul1Δ bul2Δ
+ Gln 0' 15' 45' 90' 0' 15' 45' 90'
Gap1
Put4-9myc
Dal5
Ptr2-YFP
Nce102
Protein ratio
(bul1Δ bul2Δ / bul1Δ bul2Δ pep4Δ)
1
0
*
*
**
*
0.44
0.11
0.12
0.27
Gap1 n=4
Put4 n=2
Dal5 n=4
Ptr2 n=2
C
bul1Δ bul2Δ pep4Δ
+ Gln 0' 15' 45' 90'
Gap1-GFP
Nomarski

Figure 5

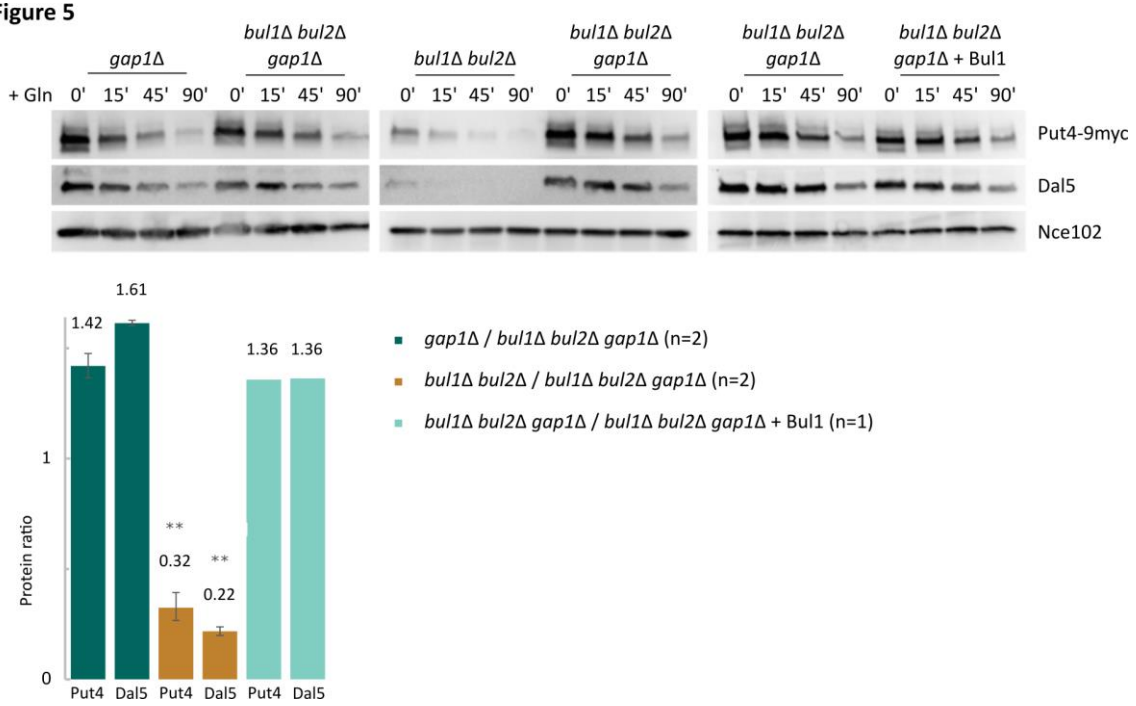

Figure 6